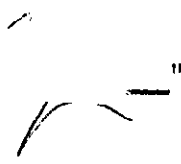


"In presenting the dissertation as a partial fulfillment of the requirements for an advanced degree from the Georgia Institute of Technology, I agree that the Library of the Institution shall make it available for inspection and circulation in accordance with its regulations governing materials of this type. I agree that permission to copy from, or to publish from, this dissertation may be granted by the professor under whose direction it was written, or, in his absence, by the dean of the Graduate Division when such copying or publication is solely for scholarly purposes and does not involve potential financial gain. It is understood that any copying from, or publication of, this dissertation which involves potential financial gain will not be allowed without written permission.



MICROWAVE SPECTRUM OF FLUOROTRICHLOROMETHANE

A THESIS

Presented to

the Faculty of the Graduate Division

By

Maurice Wayne Long

In Partial Fulfillment

of the Requirements for the Degree

Doctor of Philosophy in the School of Physics

Georgia Institute of Technology

June 1959

MICROWAVE SPECTRUM OF FLUOROTRICHLOROMETHANE

Approved:

Date Approved by Chairman:

May 11, 1959

ACKNOWLEDGEMENTS

The author is grateful to Dr. J. Q. Williams for his patience, guidance, encouragement, and support during this investigation. The guidance and helpful advice of Dr. T. L. Weatherly and the many hours that he devoted to this work will always be remembered; in addition Dr. F. K. Hurd's suggestions and interest in this investigation are appreciated. I also express appreciation to my close associate Mr. E. R. Flynt for technical assistance and many most enjoyable discussions, to Mrs. Margaret C. Bryan for patiently and cheerfully typing the thesis, and to others who have worked to make the completion of my graduate studies possible. A special note of appreciation is due to my wife, Pat, for her patience and encouragement.

TABLE OF CONTENTS

	Page
ACKNOWLEDGEMENTSiii
LIST OF TABLES	vi
LIST OF ILLUSTRATIONS.vii
Chapter	
I. INTRODUCTION	1
II. INSTRUMENTATION.	4
Sensitivity of Spectrometers	4
Detection Systems.	8
Crystal Detector and Amplifier.	8
Bolometer and Amplifier	11
Superheterodyne with Microwave Bridge	14
Results on Detection Systems.	16
Experimental Techniques Used to Investigate Fluorotri- chloromethane.	18
III. MICROWAVE SPECTRUM OF FLUOROTRICHLOROMETHANE	23
Description of Fluorotrichloromethane.	23
Molecular Rotation Theory.	25
Symmetric Rotor	25
Asymmetric Rotor.	27
Structure of Fluorotrichloromethane.	31
Nuclear Quadrupole Interaction Theory.	35
Calculations for the $J = 1 \rightarrow 2$ Quadrupole Interaction Spectrum	43

TABLE OF CONTENTS (Continued)

	Page
Experimental Results	47
J = 1→2 Spectrum	50
J = 2→3 Spectrum	56
Other Rotational Transitions	66
Quadrupole Coupling Constant	71
Discussion of Results	75
IV. CONCLUSIONS	79
V. RECOMMENDATIONS	82
APPENDICES	
A. DERIVATION FOR ADDITION OF TWO IN-PHASE WAVES	84
B. CORRECTION TO MOMENTS OF INERTIA FOR SPECIES II.	86
C. RACAH COEFFICIENTS	88
D. CALCULATIONS FOR J = 1→2 TRANSITION	90
E. PREDICTED PROMINENCES FOR J = 2→3 TRANSITION.	98
BIBLIOGRAPHY	101
VITA	104

LIST OF TABLES

Table	Page
1. Symmetry Properties of the Asymmetric Rotor Energy Levels	28
2. Observed and Predicted $J = 1 \rightarrow 2$ Transitions in Fluorotrichloromethane	31
3. Observed and Calculated Features of the $J = 1 \rightarrow 2$ Hyperfine Spectrum	54
4. Observed and Calculated Features of the $J = 2 \rightarrow 3$ Hyperfine Spectrum	61
5. Frequencies for the Strongest Line in Various Spectra.	69
6. The Quadrupole Coupling Constant of Cl^{35} in the Methyl Chlorides.	72
7. Various Chloroform Lines	74
8. Matrix Elements for $J = 1$	91
9. $J = 1, K = 1$ Eigenvalues	92
10. $J = 2, K = 1$ Eigenvalues	93
11. Intensity Factors for $J = 1 \rightarrow 2, K = 1$	94
12. Racah Coefficients Needed for Intensities.	95
13. Calculated Spectrum, $J = 1 \rightarrow 2, K = 1$	96
14. Predicted Prominences for $J = 2 \rightarrow 3, K = 1$	99
15. Predicted Prominences for $J = 2 \rightarrow 3, K = 2$	100

LIST OF ILLUSTRATIONS

Figure	Page
1. The Fluorotrichloromethane Molecule.	24
2. Graphical Description of Secular Determinants for J = 1 and for J = 2.	44
3. Predicted Quadrupole Interaction Spectrum for J = 1→2 Transition	48
4. J = 1→2 Transition in CFCl_3^{35} at 60 μ Pressure	51
5. J = 1→2 Transition in CFCl_3^{35} at 25 μ Pressure	52
6. Predicted Hyperfine Pattern, J = 2→3, K = 1	58
7. Predicted Hyperfine Pattern, J = 2→3, K = 2	59
8. J = 2→3 Transition in CFCl_3^{35} at 20 μ Pressure	60
9. J = 2→3 Transition in CFCl_3^{35} at 75 μ Pressure	63
10. Observed and Calculated Features of the J = 2→3 Transition in CFCl_3^{35}	67

CHAPTER I

INTRODUCTION

A theoretical and experimental investigation was made on the abundant symmetric top species of fluorotrichloromethane (CFCl_3). The rotational absorption lines for this molecule are very weak because the molecular dipole moment is small and because lines are split by interaction of the quadrupole moments of the three chlorine nuclei with the gradient of the electric field of the molecule. The molecular hyperfine spectra due to this interaction are very complex; the complexity increases rapidly with increase in the angular-momentum quantum number, J . For this reason the spectrum was investigated at the lowest practical frequency because of the complexity of the hyperfine structure, even though line strengths decrease rapidly with frequency. For the reasons stated above a spectrograph having optimum sensitivity was a primary objective.

Theoretical and experimental research which was devoted to the determination of optimum equipment sensitivities is discussed. Spectrographic equipment is described which was developed for operation between 8,000 mc and 18,000 mc. Little gaseous spectroscopy has been performed at these frequencies because spectroscopists have been able to find all molecular phenomena of interest at higher frequencies where line strengths are large. Use of measured sensitivity of the developed spectrograph was made to compare calculated absorption coefficients with measured values. To the best of the writer's knowledge this investigation has disclosed weaker absorption lines than ever previously reported.

A theoretical and experimental investigation of the most abundant symmetric top species of fluorotrichloromethane is discussed. No microwave data have been previously reported for this molecule. The hyperfine structure has been critically analyzed for the $J = 1 \rightarrow 2$ and $J = 2 \rightarrow 3$ transitions. The spectra occur at 9.86 kmc and 14.79 kmc, respectively. The theoretical calculation for the $J = 1 \rightarrow 2$ spectrum follows Bersohn's theory for nuclear quadrupole interaction and is similar to the work of Wolfe for the $J = 2 \rightarrow 3$ hyperfine spectrum of chloroform. The calculation results in 11 energy levels for $J = 1$ and 16 for $J = 2$; there are 99 possible transitions. The $J = 2 \rightarrow 3$ spectrum was compared with Wolfe's calculations. This work gives the quadrupole coupling constant with respect to the molecular symmetry axis, eQV_{zz} , and a centrifugal distortion constant, D_{JK} . Use of higher rotational transitions was made to assist in the analysis of the $J = 2 \rightarrow 3$ transition for fluorotrichloromethane which was particularly complex because of interference of Stark components with the hyperfine structure. The $J = 1 \rightarrow 2$ and $J = 2 \rightarrow 3$ data for $K = 1$ lines indicate that D_J is negative. Frequencies for the rotational transitions $J = 3 \rightarrow 4$ through $J = 6 \rightarrow 7$ were experimentally determined. These data indicated that D_J changes with J ; they also indicated that D_J is negative. Previous investigations for other molecules have yielded only constant positive values for D_J . The rotational constant, B , was determined by a least squares fit of $J = 1 \rightarrow 2$ through $J = 6 \rightarrow 7$ data and the value of D_{JK} obtained from the $J = 2 \rightarrow 3$ analysis.

Frequencies of the most intense lines in the $J = 1 \rightarrow 2$ transitions for CFCl_3^{35} and $\text{CFCl}_2^{35}\text{Cl}^{37}$ were used to determine the molecular structure of CFCl_3 . The data were analyzed by assuming these two molecular species to be rigid rotors.

The quadrupole coupling constant with respect to the C-Cl bond axis, eQV_{aa} , was calculated under the assumption that extranuclear charge is symmetric about the bond axis. This coupling constant is compared with those obtained from previous investigations for other methyl chlorides in gases and in solids. The calculated value for CFCl_3^{35} appears too large in comparison with the other data. The only other molecule with three nuclei of spin $3/2$ for which eQV_{aa} has been previously determined is CHCl_3^{35} ; this was determined by Wolfe from $J = 2 \rightarrow 3$ data. The $J = 1 \rightarrow 2$ hyperfine spectrum of CHCl_3^{35} was examined in the present investigation; this investigation indicated a large quadrupole coupling constant which is only slightly smaller than the value obtained for CFCl_3 . From a review of Wolfe's data and CHCl_3 data for other rotational transitions, it appears that this value of eQV_{aa} for CHCl_3 , obtained in the present investigation, is also applicable to the $J = 2 \rightarrow 3$ transition. This analysis indicated that D_J is also negative for CHCl_3 and that the magnitude depends on J .

Since the details of the measured $J = 1 \rightarrow 2$ and $J = 2 \rightarrow 3$ hyperfine spectra match the predicted spectra, the large values of eQV_{aa} obtained for CFCl_3 and CHCl_3 indicate one of the following difficulties: (1) the quadrupole interaction theory is in error by a multiplicative factor, or (2) the usual assumption of charge symmetry about the C-Cl bond is not valid for the case of three nuclei. Existence of an error in the quadrupole coupling theory might also explain large values of D_{JK} , negative values of D_J , and dependence of D_J on J .

CHAPTER II

INSTRUMENTATION

Conventional microwave spectrometers consist of a klystron, a waveguide which contains the molecules under investigation, and a video detector. The klystron is slowly swept in frequency and the detector output is recorded so as to provide molecular absorption as a function of frequency. The waveguide is constructed so that a voltage can be applied which subjects the molecules to an electric field, thereby causing splitting and shifting of absorption lines by the Stark effect. Hughes and Wilson (1) were the first to introduce the idea of using Stark modulation. The Stark modulation frequency most often used is 6 kc and is almost always between 1 kc and 100 kc. Absorption by the gas is modulated by this technique; this provides a modulated detector output which is amplified by a tuned amplifier having a center frequency equal to the modulation frequency. A phase sensitive detector is used to provide linear second detection and to further reduce bandwidth. Because the phase sensitive detector is linear and is designed to have a much narrower bandwidth than that of the tuned amplifier, the effective bandwidth for detection is equal to the bandwidth of the phase sensitive detector. The bandwidth of a phase sensitive detector can be made as small as desired by increasing the time constant of the RC output network.

Sensitivity of Spectrometers

In comparing the sensitivity of various types of microwave receivers for use in microwave spectroscopy one must recognize the basic

differences in the types of signals which are detected and amplified. In many applications the signal consists of a weak pulse of microwave power. In microwave spectroscopy the signal is in the form of a small decrement in a relatively large amount of power. A decremental signal which varies in power by the amount ΔP can be represented as the sum of a relatively large signal of power P and weak periodic pulses of power P' which are in phase with the large signal. Let P' represent the peak power of the weak pulses. The derivation in Appendix A shows that

$$P' = \frac{(\Delta P)^2}{4P}$$

provided that P' is much smaller than P . The problem of calculating the minimum detectable decrement of power in microwave spectroscopy can then be accomplished by calculating the minimum detectable pulses having power P' . The minimum noise power, that due to Johnson noise, referred to the input of a receiver is

$$P_n = kT\Delta\nu$$

where $\Delta\nu$ is the effective bandwidth. At room temperature this becomes

$$P_n = 4 \times 10^{-21} \Delta\nu \text{ watts.}$$

If the minimum detectable signal is defined as the signal having power P' equal to noise power P_n , the minimum detectable decrement of power is

$$\Delta P_{\min} = 2\sqrt{P P_n} = 1.26 \times 10^{-10} \sqrt{P\Delta\nu} \text{ watts.}$$

ΔP in terms of the absorption coefficient of the gas, γ , for a cell length L can be approximated as

$$\Delta P = \gamma L P.$$

Therefore the minimum detectable absorption coefficient is

$$\gamma_{\min} = \frac{1.26 \times 10^{-10}}{L} \sqrt{\frac{\Delta \nu}{P}}.$$

Under the assumption that $\Delta \nu$ is 0.01 cps, P is 10^{-3} watt and L is 350 cm, the minimum detectable absorption coefficient is about 10^{-12} cm^{-1} . The example cited above assumed noiseless components, a very narrow but usable pass band, a somewhat higher power P than is normally used and a typical cell length. A greater cell length was not used because substantial improvement in minimum detectable absorption coefficient would result only through use of very unwieldy lengths. The above equations show the well-known fact that any sensitivity is available if one is willing to restrict $\Delta \nu$ to a small enough value. This means that the response time of the system must become very long and the data-taking time accordingly lengthened.

Large effective lengths are theoretically obtainable by the use of cavity type absorption cells (2). These cells are not discussed because a suitable means for applying a Stark field to a high-Q cavity was not found.

Based on a graph given by Townes and Schawlow (3), 95 percent of all lines reported between 20,000 and 30,000 mc have intensities greater than 10^{-7} cm^{-1} . Since intensities of microwave lines increase with fre-

quency approximately as ν^3 , equipment capable of detecting lines having absorption coefficients as weak as 10^{-9} cm^{-1} should be suitable for most research down to 3000 mc. As far as we know, the weakest line measured prior to this research is from CF_3I and reported by Sterzer (4). He calculated an intensity at room temperature of $3.3 \times 10^{-10} \text{ cm}^{-1}$ for his weakest line which occurred at about 3400 mc. The weakest line reported in this investigation for the $J = 1 \rightarrow 2$ rotational transition of CFCl_3 has a calculated intensity at room temperature of less than 10^{-10} cm^{-1} .

One of the most promising methods for detecting microwave power is the coherent first detector. This detector (5, 6) is like the superheterodyne detector with the exception that the local oscillator frequency is derived from the same source as the incoming signal. If these two signals are in phase, the equation representing detection is the same as that for the superheterodyne having an intermediate frequency of zero; the amplifier following the detecting element is tuned to the repetition frequency of the signal pulses. Richmond (7) reported minimum detectable signals of 0.5×10^{-12} watt using X-band bolometers or crystals with a 4-cps pass band. Use of coherent first detectors represents a major step in the improvement of sensitivity over video detection techniques.

It is interesting to compare the coherent first detector with the conventional Stark modulation scheme used in spectroscopy. The signal out of the Stark cell is represented in Appendix A as two signals of the same frequency. Thus it can be seen that the conventional Stark system which is often referred to as a video system is in actuality a coherent first detector, simply a superheterodyne which has zero intermediate

frequency. Once it is recognized that the Stark system is a superheterodyne, spectrometers can be analyzed by using known results for the superheterodyne.

Stark cells are usually constructed out of standard waveguide having as large a cross-section area as practicable; this is for the purpose of minimizing power density. Reduction of power density permits higher spectrometer sensitivity because higher signal powers can be used for equal broadening of lines due to power saturation. The Stark electrode consists of a conducting sheet which is isolated from the waveguide by insulating tape. The conducting sheet runs the length of the waveguide cell and is mounted parallel to the broad side of the waveguide. Ratios of width to height of standard waveguides are approximately 2:1. For this reason Stark-cell capacitance is not strongly dependent on waveguide size. In general the cross-sectional area of Stark cells will be increased with increase in wavelength. On this basis a larger Stark voltage will be required across the cell for a given electric field strength at a lower frequency than at a higher frequency. The higher power requirements for Stark modulators can be offset by the use of low Stark modulation frequencies. The bolometer detector provides a sensitive means for using low modulation frequencies.

Detection Systems

Crystal Detector and Amplifier.--Crystal rectifiers are used almost exclusively for detectors of microwaves in spectroscopy. Though the rectifying properties vary from crystal to crystal, their characteristics can be roughly divided into a square-law region where the rectified current I is proportional to P (holds for $P < 10^{-5}$ watts) and the linear

region where I is proportional to \sqrt{P} (holds for $P > 10^{-4}$ watts).

In spectrometers the resonance signal usually appears as a small modulation of a comparatively large carrier reaching the detector. Because of the carrier, a rectified current flows in the crystal. This current produces a frequency dependent noise which can be represented (8), in the square-law region, by

$$P_n = \left(\frac{\beta P^2}{f} + 1 \right) kT \Delta\nu$$

where f is the frequency around which the pass band $\Delta\nu$ is centered and where

$$\beta \approx 5 \times 10^{14} \text{ watt}^{-2} \text{ sec}^{-1}$$

for the type 1N23C crystal. The conversion gain in the square-law region can be represented by $G = SP$ where S was found for the 1N23C crystal to be approximately 500 watt^{-1} . For signal levels such that crystal noise greatly exceeds amplifier noise, crystal noise is proportional to P^2 . The change in power in the output of the Stark cell is proportional to P and consequently, since the crystal output power is proportional to the square of the input power, the signal within the amplifier also varies as P^2 . Thus for small variations of the input power such as is produced by gas absorption, the minimum detectable gas absorption coefficient is independent of power within the Stark cell provided this power is sufficiently large to produce crystal noise greatly exceeding amplifier noise and sufficiently small so that the crystal is operating in its square-law region.

As the carrier power reaching the detector is increased, P_n increases. However when the input power is a few tenths of a milliwatt, the crystal behaves as a linear detector and, in spite of the additional noise, becomes more sensitive than it is as a square-law detector. Because of the increase in noise and increase in backward current through the crystal, the sensitivity decreases as the input power exceeds a few milliwatts. From the theory of superheterodyne receivers it is known that the detector output voltage due to a small pulsed signal is always proportional to the incident electric field of this signal provided the large signal is much greater than the small signal. Therefore, regardless of whether the crystal is behaving as a linear detector or a square-law detector, the output voltage is proportional to \sqrt{P} and consequently the output voltage of a spectrometer is always proportional to ΔP provided the system is linear beyond the first detector.

The noise power of a crystal in the linear region can be represented by (8)

$$P_n = \left(\frac{\gamma P}{f} + 1\right) kT \Delta \nu$$

where $\gamma \approx 10^{11}$ watt⁻¹ sec⁻¹ for a type LN23C crystal. The conversion gain G of a type LN23C crystal in the linear region is approximately 0.3. This equation yields a noise power of 4.8×10^{-18} watt per cycle of bandwidth at 85 kc for one milliwatt incident upon the crystal. Using the value of 0.3 for conversion gain, minimum detectable P' is 16×10^{-18} watt. The detectable decrement of power at one milliwatt level is then

$$P' = 16 \times 10^{-18} = \frac{(\Delta P)_{\min}^2}{4 \times 10^{-3}}$$

or

$$(\Delta P)_{\min} = 2.5 \times 10^{-10} \text{ w}$$

for 1 cps bandwidth. Measurements using the Georgia Institute of Technology 85-kc spectrometer and a type 1N23E crystal indicated agreement, within experimental error, with this value of $(\Delta P)_{\min}$ when normalized for a 1 cps bandwidth. This result indicates

$$(\Delta P)_{\min} = 2.4 \times 10^{-9} \text{ w}$$

with 1 cps bandwidth and a 1-kc system operating at the one milliwatt level.

The internal impedance of crystal rectifiers is of the order of thousands of ohms in the square-region and is reduced with increase in incident power. In the linear region this impedance is down to several hundred ohms. Because of the high impedance in the square-law region, input circuits for spectrometers usually have a high impedance at the modulation frequency; this is often accompanied by too-large a d-c resistance for crystal current. In order to minimize noise and conversion loss when operating in the linear region, the d-c resistance (9) external to the crystal should be reduced to less than 100 ohms.

Bolometer and Amplifier.--The bolometers discussed in this section are commercially available detecting elements which consist of short lengths

of wire of low thermal time constants. The useful property of these elements is that resistance is a function of the amount of power absorbed. Bolometers are normally biased with direct current to an operating resistance of 200 ohms; the addition of r-f power to the element increases the element resistance above this bias point. Analyses of detector sensitivities using bolometers are easier than for crystals because bolometer noise is essentially independent of microwave power. Theoretically the noise is that of a 200 ohm resistor at the elevated temperature, due to the bias current, of the bolometer. Based on typical sensitivities in ohms per milliwatt and an operating temperature consistent with typical temperature coefficients of expansion, an estimate (10) of minimum detectable change in power is

$$\Delta P = 10^{-10} \sqrt{\Delta \nu} \text{ watt.}$$

Recall that the minimum ΔP for a 1-kc system using the type 1N23C crystal operating at a one milliwatt level is

$$\Delta P = 2.4 \times 10^{-9} \sqrt{\Delta \nu} \text{ watt.}$$

Because the noise from a bolometer is that of a resistance at an elevated temperature, bolometer noise is of the order of Johnson noise. For this reason low noise amplifiers are required for use with bolometers. On the other hand, the noise power of crystals at frequencies in the kilocycle region is thousands of times Johnson noise and consequently amplifier noise figure is of less importance. For the same reasons, klystron noise is of more importance when using bolometers. The above considera-

tion is not applicable to conventional microwave superheterodyne receivers employing intermediate frequencies in the megacycle region.

A 1-kc spectrograph has been constructed for determining pitfalls associated with bolometer systems. Modulation frequencies must be low because of bolometer thermal time constants; 1 kc is sufficiently low for most bolometers. This frequency was selected so that commercially available low-noise detector amplifiers could be employed. The work required the design and construction of a phase sensitive detector, recorder amplifier, and 1-kc Stark modulator.

Minimum detectable signals were first determined by measuring 1-kc square wave pulses from a klystron. By interchanging commercial amplifiers, differences of 15 db after normalizing to a specific bandwidth were measured for minimum detectable signals with so-called low-noise amplifiers. This was particularly disturbing because minimum detectable signal level with a square law detecting element varies as the square root of noise figure; this indicated noise figures differing by a factor of 1000. The amplifier giving the best performance was improved by using a d-c heater supply and battery bias for the bolometer. The amplifier noise figure appears to be less than 2 with this arrangement.

Minimum detectable signal with the best amplifier and many commercial bolometers was measured. The better bolometers, Narda type N-610B, gave minimum detectable signals corresponding to

$$\Delta P = 4 \times 10^{-10} \sqrt{\Delta \nu}.$$

This result is encouraging in that it provides a minimum ΔP which is only a factor of 4 greater than the theoretical value.

The next problem with the bolometer system was klystron noise; little data exist on this noise. It was found that an X-12 klystron operating at 15 kmc and delivering 2-3 milliwatts to the bolometer doubled bolometer plus amplifier noise. Comparable noise was observed with the two available X-12 klystrons. X-13 and X-13B klystrons in the 10 kmc region contributed almost negligible noise to the system when delivering 2-3 milliwatts to the bolometers.

Superheterodyne with Microwave Bridge.--Initial investigations on equipment sensitivity were devoted to the conventional superheterodyne receiver having an intermediate frequency in the megacycle region. The advantage of a high intermediate frequency is the reduction of crystal noise because of its $1/f$ dependence. At higher frequencies where detector power must be small to avoid molecular saturation, the superheterodyne provides a means for operating crystals at high enough power levels to obtain minimum conversion loss.

Conventional superheterodyne detection requires an auxiliary oscillator which is kept at a constant frequency difference from the signal generator. This local oscillator may be made to follow the signal oscillator by a discriminator and automatic frequency-control system. The need for a local oscillator signal makes the superheterodyne more complicated than the simple detector using a crystal or bolometer. Moreover the local oscillator may be an additional source of noise, although most of this noise can be eliminated by the use of a balanced mixer. To reduce the carrier relative to the useful signal, a balanced bridge is required. This bridge permits the use of superheterodyne detection without overloading the intermediate frequency amplifiers and will reduce the signal oscillator noise.

Little information could be found in the literature regarding actual sensitivities that have been obtained with superheterodyne detectors in microwave spectrometers, although Townes and Schawlow do indicate (11) that sensitivities on the order of 10^{-9} cm^{-1} have been obtained. In pursuance of the present research, an X-band bridge was constructed and used with an existing i-f amplifier modified for the present application. The center frequency of the i-f amplifier is 140 mc and the bandwidth is 40 mc. Use of the wide bandwidth amplifier removes the need for an afc as long as searching is restricted to narrow frequency limits. The noise figure of the amplifier is 10 db; this is a large noise figure, but it was considered suitable for indoctrination into problems associated with bridge type superheterodyne systems. Results of this work were discouraging in that the sensitivities obtained were seriously limited by available bridge stabilities and the many other complicating features of such a system. Sensitivities over short time intervals were comparable to those obtained with the 85-kc crystal system operating at a one milliwatt level but because of many types of instabilities the practical limit on sensitivity was less than with the 85-kc crystal system. Use of a less noisy i-f amplifier would improve the system sensitivity, but the resulting improvement would not be adequate to justify the use of the superheterodyne system. After this rather frustrating attempt to obtain high sensitivities, the work of Misra (12) on sensitivity of paramagnetic resonance spectrometers was discovered. Although it is believed that his choice of a superheterodyne system for high sensitivity was based on erroneous analyses of

crystal and bolometer systems, his thesis vividly displays problems which are encountered in attempts to use this type of spectrometer. The availability of high detector powers for gaseous spectroscopy in the 4 to 16 kmc region through the use of absorption cells having large cross-sectional areas and the necessity for frequency tuning of the detection system makes the practical application of bridge type superheterodyne systems even more unlikely than in the field of paramagnetic resonance. One of the major problems that would have to be overcome is the development of a suitably linear second detector. This problem is serious because of the large ratio of required i-f bandwidth, because of short term local oscillator instabilities, to video bandwidth. The effective noise bandwidth for a square-law detector is $\sqrt{f_1 f_2}$, where f_1 represents the intermediate frequency and f_2 represents the narrow video bandwidth preceding the recorder. Conventional diode detectors when operated under optimum conditions are good linear detectors, but still some loss in effective noise bandwidth is expected because of the large ratio of f_1 to f_2 required.

Results on Detection Systems.--Based on a pass band of one cycle per second, a spectrograph employing noiseless components, an ideal second detector, and a Stark cell of reasonable length would have a noise level corresponding to an absorption coefficient of 10^{-11} cm⁻¹. Analysis shows that the conventional Stark spectrograph introduced by Hughes and Wilson in 1947 is equivalent to the coherent first detector. This detector, which is analogous to the superheterodyne having an intermediate frequency of zero, is today considered to be one of the most promising methods for detecting microwave power.

Because of the similarity of the Stark spectrograph to the superheterodyne, greatest sensitivity can be achieved with crystal diodes and bolometers if operated at higher microwave power levels than is usually used with spectrographs. At these power levels, a Stark cell having a large cross-sectional area is required to prevent molecular saturation. The noise power of crystal diode detectors varies inversely with Stark modulation frequency. The measured noise level of an 85-kc Stark spectrograph operated in this manner corresponds to an absorption coefficient of $6 \times 10^{-10} \text{ cm}^{-1}$ for a one cycle per second pass band. Under similar operating conditions but with a 1,000 cps modulation frequency, the best sensitivity obtained with a bolometer system corresponds to an absorption coefficient of 10^{-9} cm^{-1} .

In general greater Stark modulator power is required at the lower microwave frequencies to provide comparable Stark fields because larger waveguide is used. The higher power requirements for Stark modulators can be offset by the use of the low Stark modulation frequencies suitable for bolometers. Based on the $1/f$ dependence of noise power for crystal diodes, the noise level of a crystal diode system operating with a 1,000 cps modulation frequency is expected to have a noise level corresponding to an absorption coefficient of $6 \times 10^{-9} \text{ cm}^{-1}$ for a one cycle per second pass band.

The superheterodyne detector with intermediate frequency in the megacycle region provides a means for reducing crystal noise because of the $1/f$ dependence. Conventional superheterodyne detection requires an auxiliary oscillator which is kept at a constant frequency difference

from the signal generator. The need for such a local oscillator signal makes the superheterodyne more complicated than the simple detector using a crystal or bolometer. Moreover the local oscillator may be an additional source of noise, although most of this noise can be eliminated by the use of a balanced mixer. Also, a balanced microwave bridge is required to reduce the carrier relative to the useful signal. The instabilities and sources of noise introduced from the additional components substantially limit system performance. Under the most suitable conditions, measured sensitivities never exceeded the value obtained with the simple crystal and tuned amplifier operating at 85 kc. The superheterodyne in conjunction with the microwave bridge does, however, provide a means for operating crystals at high enough power levels to obtain minimum conversion loss without subjecting the sample molecules to high power levels.

Ninety-five percent of all lines reported between 20,000 and 30,000 mc have intensities greater than 10^{-7} cm^{-1} . Since intensities of microwave lines vary with frequency approximately as frequency cubed, equipment capable of detecting lines having absorption coefficients as weak as 10^{-9} cm^{-1} should be suitable for most research down to 3,000 mc. A simple crystal diode system was used in this research to measure very weak absorption lines which occur at about 9850 mc; the absorption coefficients are approximately 10^{-10} cm^{-1} .

Experimental Techniques Used to Investigate Fluorotrichloromethane

The spectrometer used in the investigation of CFCl_3 consists of a conventional Stark-modulation system (13), modified for use with relatively high power incident upon the crystal diode detector. This system

employs an 85-kc square-wave modulator which applies an electric field in the waveguide region occupied by the gas. The applied square-wave voltage is clamped so that it alternates between zero and an adjustable negative voltage. The square wave can readily be unclamped so that it swings with equal positive and negative potentials. This provides a test as to whether or not an output deflection is actually an absorption line. Second detection is accomplished by a phase sensitive detector with an output network having a time constant of several seconds.

The input circuit of the pre-amplifier was modified to reduce the d-c resistance for crystal current; this minimizes noise and conversion loss for high power operation (see section entitled Crystal Detector and Amplifier). The modification consists of replacing the 125 mh choke coil and 1000 ohm resistor which shunts the diode input shown on page 60 of reference 13 with a 10 mh ferrite core coil having a resistance of 28 ohms. The microwave power for measuring the lower transitions was usually such that the rectified crystal current* was between one-half and two milliamperes, corresponding to a few milliwatts of microwave power. Objectionable 85-kc pickup was found to exist as a result of current flow along the walls of the Stark cell and to the crystal detector through the crystal holder. The pick-up was removed by isolating the crystal holder from the cell by using a thin Mylar spacer between waveguide flanges and Nylon connecting screws.

*This measurement was made with a low resistance meter, so that the measured current is essentially the short-circuit current.

Microwave power is supplied by reflex klystrons which were slowly swept through the frequency range of interest by mechanically tuning with one of several slow speed motors and a variable speed gear reducer.

The X-band cell has inside cross-sectional dimensions of 0.900 inch by 0.400 inch and was made with the general fabrication techniques used with the S-band cell described below. The X-band cell is, however, made of two sections and has a total length of 20 feet. The S-band cell consists of a 0.040 inch by 140 inches brass sheet for a Stark electrode mounted in a 12-foot length of waveguide. The guide is standard type RG48/U which has inside cross-sectional dimensions of 2.84 inches by 1.34 inches. Each side of the electrode is supported by 93-mil Teflon tape. To minimize interface reflections of the microwaves, the ends of the Teflon tape and Stark electrode are tapered. The cell is sealed at each end by a 10 mil Mylar window compressed with an O-ring between waveguide flanges. A gas port is located at each end for passing gas through the cell. The ports consist of 4-inch slits having a width of $1/8$ inch. Standard $1/2$ -inch copper tubing is used for connecting the cell to the gas handling system. A wooden framework lined with polyfoam encloses the cell. This serves as a heat insulator to facilitate cooling the cell with dry ice.

For measurements on each transition, microwave power is divided into two parts: one portion is supplied to a crystal diode associated with the frequency measuring system, where its frequency is determined approximately by a wavemeter and then more precisely by comparison with standard markers from a secondary frequency standard. The remainder of the power passes through the absorption cell to a second crystal diode which serves as a detector.

A crystal controlled secondary frequency standard compared with WWV generates standard microwave frequencies 30 mc apart at the terminals of a crystal diode. Beat frequencies are also produced in this diode which are the differences between the standard frequencies and the unknown klystron frequency. These are detected by a National HRO receiver. Absorption lines are observed by two methods. For the $J = 1 \rightarrow 2$ and $J = 2 \rightarrow 3$ transitions a long time constant RC network was used at the output of the phase sensitive detector. Because of this the klystron frequency was slowly varied and the spectrograph output was indicated on a chart recorder. For the higher transitions the klystrons were swept in frequency by applying a sawtooth voltage to the repeller at a rate of 15 cps; sometimes the chart recorder was used to study line detail. The recorded $J = 1 \rightarrow 2$ and $J = 2 \rightarrow 3$ spectra were calibrated in frequency by manually actuating the side pin of the chart recorder at intervals of one megacycle, as determined by listening for a beat note between the frequency standard and the mechanically swept klystron on the HRO receiver. More accurate frequency determinations were made for the major prominences by measuring the difference frequency at the time that the recorder indicated a peak signal. To reduce errors resulting from long filter time constants, the frequency obtained for increasing klystron frequency was averaged with that obtained for decreasing klystron frequency. The reported frequencies are averages of repeated measurements of this type and the ranges indicated for the measurements are probable errors associated with the ensemble of frequency determinations for a single prominence under the assumption that frequency differences are normally distributed about their means. For

the higher transitions the klystron frequency was swept electronically and the absorption line displayed on an oscilloscope. Frequencies were determined by superimposing a difference frequency marker on the observed absorption line and averaging data for sweeping the klystron up in frequency with that for sweeping the klystron down in frequency.

Major components used in observing data for each rotational transition are listed below.

<u>Transition</u>	<u>Frequency (kmc)</u>	<u>Klystron</u>	<u>Stark Cell</u>	<u>Crystal</u>
1→2	9.86	X-13	S-band	1N23E
2→3	14.79	X-12	S-band	1N78B
3→4	19.73	QK-306	X-band	1N26
4→5	24.66	2K33	X-band	1N26
5→6	29.59	QK-289	X-band	1N26
6→7	34.52	QK-291	X-band	1N26.

The Stark cell was kept at dry ice temperature by filling the insulated framework with dry ice. The sample CFCl_3 was cooled by surrounding the sample holder with a dry ice and acetone solution contained in an insulated flask. The sample holder was connected to the input port of the Stark cell through two stopcocks separated by a small volume consisting of a short section of glass tubing. Gas was introduced into the small volume by opening and closing the stopcock closest to the sample holder with the other stopcock closed. The second stopcock was then opened and closed, providing a Stark cell pressure suitable for high pressure operation. Lower pressures were obtained by removing gas from the output port with a diffusion pump.

CHAPTER III

MICROWAVE SPECTRUM OF FLUOROTRICHLOROMETHANE

Description of Fluorotrichloromethane

The fluorotrichloromethane employed as a sample in this investigation was purchased from The Matheson Company, Inc. This gas, which has the trade name of "Freon 11", has a purity of 99.9 percent. A sketch of the molecule is shown in Figure 1.

Isotopic abundances and nuclear spins for C, F, and Cl follow (13):

<u>Element</u>	<u>Mass Number</u>	<u>Abundance (percent)</u>	<u>Nuclear Spin</u>
C	12	98.88	0
	13	1.12	1/2
F	19	100	1/2
Cl	35	75.4	3/2
	37	24.6	3/2

Nuclear quadrupole moments, through interaction with the gradient of the electric field, contribute a hyperfine structure to the rotational spectrum. It is well established that there is no electric quadrupole moment for nuclei with spin 0 or 1/2. Therefore it is expected that the only nuclear multipole moments which need to be considered are the electric quadrupole moments of the three chlorine atoms.

Since the natural abundance ratio $\text{Cl}^{35}:\text{Cl}^{37}$ is approximately 3:1, one has the following abundances for the four species of fluorotrichloromethane:

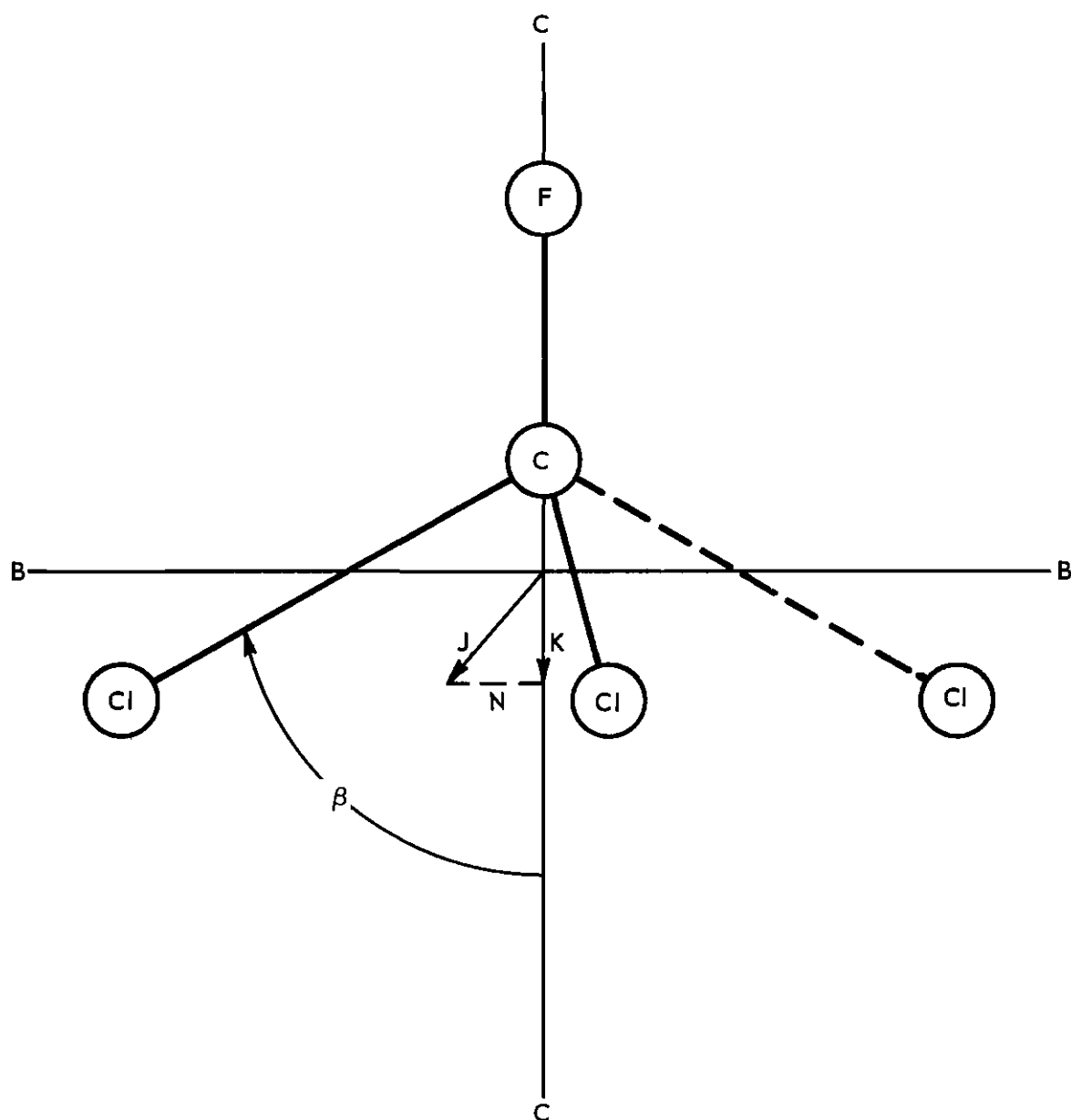


Figure 1. The Fluorotrichloromethane Molecule.

Species I	CFCl_3^{35}	27/64
Species II	$\text{CFCl}_2^{35}\text{Cl}^{37}$	27/64
Species III	$\text{CFCl}_2^{35}\text{Cl}^{35}$	9/64
Species IV	CFCl_3^{37}	1/64.

Molecular Rotation Theory

Symmetric Rotor.--Symmetric-top molecules have equal moments of inertia about two of their three principal axes. The total angular momentum is constant in magnitude as well as in direction, and its component in the direction of the symmetry axis is constant in magnitude. The symmetry axis rotates at a constant angle and at a constant frequency about the total angular momentum vector.

The quantum mechanical solution for the rotational energies of a rigid symmetric-top molecule can be expressed as

$$E = \frac{J(J+1)\hbar^2}{2I_B} + \frac{1}{2} \left[\frac{1}{I_C} - \frac{1}{I_B} \right] \hbar^2 K^2$$

where I_C is the moment of inertia about the symmetry axis, and $I_B (=I_A)$ is the moment of inertia about the other two perpendicular principal axes. J is the total angular momentum quantum number, and K is the component of angular momentum along the symmetry axis.

The above equation applies to a rigid molecule. For a non-rigid molecule corrections must be applied for centrifugal distortion. It is usual to express these corrections in terms of the distortion coefficients D_J , D_K , and D_{JK} . The energies of a non-rigid symmetric top molecule are given by

$$\frac{E}{h} = BJ(J+1) + (C-B)K^2 - D_J J^2(J+1)^2 - D_{JK} J(J+1)K^2 - D_K K^4$$

where

$$B = \frac{h}{8\pi^2 I_B}, \quad C = \frac{h}{8\pi^2 I_C}.$$

Because of the symmetry there can be no dipole moment component perpendicular to the symmetry axis, and hence the electric fields associated with radiation cannot exert a torque about this axis. Therefore for electric dipole radiation one has the selection rule $\Delta K = 0$. The selection rule for the quantum number J for electric dipole radiation is the usual $\Delta J = 0, \pm 1$. Therefore, the frequencies of the absorption lines for the $J \rightarrow J + 1$ rotational transitions are given by

$$f = 2(J+1)(B - D_{JK}K^2) - 4D_J(J+1)^3.$$

Because D_J and D_{JK} are small constants a series of almost equally spaced absorption lines, separated by $2B$, is to be expected.

The main effect of the centrifugal distortion is to remove the degeneracy of the different K states. Without the distortion only one line would appear for each different transition of the principal quantum number, J , because of the $\Delta K = 0$ selection rule.

The two symmetric isotopic species of CFCl_3 contain three identical chlorine nuclei which interact with the average gradient of the electric field produced by the rest of the molecule. This interaction is sufficiently large to produce a hyperfine structure. The frequencies

of the absorption lines for the $J \rightarrow J+1$ rotational transition including the effect of quadrupole interaction may be expressed as

$$f = 2(J+1)(B-D_{JK}K^2) - 4D_J(J+1)^3 + \Delta\nu_Q. \quad (1)$$

All terms in Equation 1 are defined above with the exception of $\Delta\nu_Q$, which represents the frequency shift resulting from nuclear quadrupole interaction.

Asymmetric Rotor. --The allowed rotational energies of an asymmetric top molecule ($I_A < I_B < I_C$) are considerably more difficult to obtain than are those for linear and symmetric-top molecules (14). The energies for asymmetric rotors can be expressed in closed form for low values of J only. There are $2J+1$ sub-levels of energy for each J of an asymmetric top. These are labeled J_τ where τ takes on $2J+1$ integral values ($-J \leq \tau \leq J$). The sub-levels are numbered in order of increasing energy, the lowest level being J_{-J} and the highest level being J_{+J} .

Symmetry properties of the levels J_τ can be specified (14) in terms of the behavior of the corresponding wave functions with respect to rotations by π about the C axis (C_{2C}) and about the A axis (C_{2A}). These properties, with the corresponding values of K for the prolate and oblate limiting cases are given in Table 1.

Species I and IV of fluorotrichloromethane, being symmetric tops, have their permanent electric dipole moments along the C axis. Therefore, it is expected that the slightly asymmetric top resulting from the substitution of a different isotope for one species will still have its permanent dipole moment lying almost along the C axis. In addition to

Table 1. Symmetry Properties of the Asymmetric Rotor Energy Levels

J	τ	K(prolate)	K(oblate)	C_{2C}	C_{2A}
2	2	2	0	+	+
	1	2	1	-	+
	0	1	1	-	-
	-1	1	2	+	-
	-2	0	2	+	+
1	1	1	0	+	-
	0	1	1	-	-
	-1	0	1	-	+
0	0	0	0	+	+

the selection rule $\Delta J = 0, \pm 1$, the symmetry selection rules for this case are (14)

$$+ + \longleftrightarrow + - \text{ and } - + \longleftrightarrow --.$$

For the energy levels shown in Table 1, these selection rules correspond to ΔK (oblate) = 0. The energies, E_{τ}^J , for the states listed in Table 1 are:

$$E_2^2/h = 2A + 2B + 2C + 2 \sqrt{(B-C)^2 + (A-C)(A-B)}$$

$$E_1^2/h = 4A + B + C$$

$$E_0^2/h = A + 4B + C$$

$$E_{-1}^2/h = A + B + 4C$$

$$E_{-2}^2/h = 2A + 2B + 2C - 2 \sqrt{(B-C)^2 + (A-C)(A-B)}$$

$$E_1^1/h = A + B$$

$$E_0^1/h = A + C$$

$$E_{-1}^1/h = B + C$$

$$E_0^0/h = 0.$$

From these values of energy and the selection rules, the frequencies corresponding to the $J = 1 \rightarrow 2$ transitions in Species II and III are:

$$f(\tau = 1 \rightarrow 2) = A + B + 2C + 2 \sqrt{(B-C)^2 + (A-C)(A-B)}$$

$$f(\tau = 0 \rightarrow 1) = 3A + B$$

$$f(\tau = -1 \rightarrow 0) = A + 3B.$$

For slightly asymmetric tops the centrifugal distortion effects are approximately the same as for the symmetric top. Because of this, effects of centrifugal distortion need not be considered in determining the molecular structure which was obtained from $J = 1 \rightarrow 2$ transition data for species I and species II.

Wolfe (15) has shown that the most intense nuclear quadrupole hyperfine structure component for the transition $J \rightarrow J + 1$, in a molecule with three identical quadrupolar nuclei of spin $3/2$, has $K = 1 \rightarrow 1$. His expression for frequency, when modified to be in terms of the quadrupole coupling constant eQV_{zz} (see section entitled Nuclear Quadrupole Interaction Theory), is

$$\Delta\nu_Q = \beta(J) eQV_{zz}.$$

$\Delta\nu_Q$ is the frequency by which the most intense hyperfine component of the $J \rightarrow J + 1$ transition is shifted because of quadrupole interaction. To account for the shift in the most intense component of species II, an effective nuclear quadrupole coupling constant is employed,

$$(eQV_{zz})_{\text{effective}} = \left[N_{35} + N_{37} (Q^{37}/Q^{35}) \right] \frac{eQV_{zz}}{3}.$$

Here N_{35} is the number of Cl^{35} nuclei in the molecule, N_{37} is the number of Cl^{37} nuclei. From the work of Livingston (16), $Q^{37}/Q^{35} = 0.788$.

Therefore, for species II

$$(eQV_{zz})_{\text{effective}} = \left[2 + 1(0.788) \right] \frac{eQV_{zz}}{3} = 0.929 eQV_{zz}.$$

Structure of Fluorotrichloromethane

The structure of fluorotrichloromethane was determined from experimental $J = 1 \rightarrow 2$ data for the most intense line of species I and the most intense lines of the transitions $J_{\tau} = 1_0 \rightarrow 2_1$ and $J_{\tau} = 1_{-1} \rightarrow 2_0$ for species II.

Results given in the section on experimental data indicate that the most intense line in the $J = 1 \rightarrow 2$ spectrum for species I is lowered by 2.26 mc, i.e.,

$$\Delta\nu_Q(\text{I}) = -2.26 \text{ mc.}$$

Based on $(eQV_{zz})_{\text{effective}}$ and $\Delta\nu_Q(\text{I})$ it is expected that the most intense lines of the various transitions for species II are shifted by

$$\Delta\nu_Q(\text{II}) = -2.10 \text{ mc.}$$

Relatively low Stark fields (about 160 volts/cm) were employed throughout this investigation. As a consequence, $K = 0$ components were not observed since these possess no first-order Stark effect. The available Stark field was not large enough to observe the frequency $f(1_1 \rightarrow 2_2)$, which corresponds to $K = 0$ in the limiting case of a symmetric top. Table 2 gives the observed frequencies and corresponding frequency expressions in terms of rotational constants.

Table 2. Observed and Predicted $J = 1 \rightarrow 2$ Transitions in Fluorotrichloromethane

Species	$f(\text{Observed})$	$f(\text{Predicted})$
I	$9859.30 \pm 0.04 \text{ mc}$	$4B(\text{I}) - 2.26 \text{ mc}$
II	$9786.05 \pm 0.20 \text{ mc}$	$3A(\text{II}) + B(\text{II}) - 2.10 \text{ mc}$
	$9656.62 \pm 0.10 \text{ mc}$	$A(\text{II}) + 3B(\text{II}) - 2.10 \text{ mc}$

The data in Table 2 yield

$$A(I) = B(I) = 2465.39 \text{ mc}$$

$$A(II) = 2463.22 \text{ mc}$$

$$B(II) = 2398.50 \text{ mc.}$$

The relation

$$I_A (A^2 \text{Amu}) A(\text{mc}) = 5.05531 \times 10^5$$

was employed to convert between moments of inertia and rotational constants.

Based on the following atomic masses,

$$\text{F:} \quad 19.00450$$

$$\text{C}^{12}: \quad 12.00382$$

$$\text{Cl}^{35}: \quad 34.97867$$

$$\text{Cl}^{37}: \quad 36.97750,$$

the principal moments of inertia, in units of Angstroms-squared times atomic mass units, are:

Species I:

$$I_A = I_B = I_{xx} = I_{yy} = 52.46801 a^2 + 16.34774 b^2 + 29.33931 ab \cos \beta \\ - 28.53255 a^2 \cos^2 \beta$$

$$I_C = I_{zz} = 104.93601 a^2 \sin^2 \beta$$

Species II:

$$I_A = I_{xx} - \Delta, \text{ where}$$

$$I_{xx} = 52.46801 a^2 + 16.38624 b^2 + 29.46494 ab \cos\beta \\ - 28.43006 a^2 \cos^2\beta,$$

$$\Delta = \frac{I_{xz}^2}{(I_{zz} - I_{xx})},$$

$$I_{xz} = -0.27538 ab \sin\beta - 0.44932 a^2 \sin\beta \cos\beta,$$

and

$$I_{zz} = 106.90588 a^2 \sin^2\beta.$$

$$I_B = I_{yy} = 54.43787 a^2 + 16.38624 b^2 + 29.46494 ab \cos\beta \\ - 30.39993 a^2 \cos^2\beta.$$

In these equations a and b are the C-Cl and C-F bond distances, respectively, and β is the angle between a C-Cl bond direction and the symmetry axis, z . For species I, the C axis is parallel to the C-F bond, with the A and B axes arbitrary but perpendicular to each other and to C. For species II, the C axis lies almost parallel to the C-F bond, in the plane C-F-Cl³⁷. The A axis is in this plane and is perpendicular to C. The B axis lies perpendicular to the plane of A and C.

The term Δ is an approximate correction to I_A due to the tipping of axis C in the asymmetric species (see Appendix B). For the structural parameters involved

$$\Delta = 0.0115 A^2 \text{ Amu},$$

and I_{xx} is approximately $205 A^2 \text{ Amu}$.

The structure was determined from the moments of inertia calculated from experimental data: $I_A(I)$, $I_A(II)$, and $I_B(II)$. Substitution of $I_A(II)$ into $I_B(II)$ with $\Delta = 0.0115$ yields a value for \underline{a} as a function of β ; this relation was used to eliminate \underline{a} from $I_A(I)$ and $I_B(II)$. Values of \underline{b} were then obtained from the equations for $I_A(I)$ and $I_B(II)$ for assumed values of β . The solution for β was selected as the value which results in equal values of b from these equations. β was determined to be $70^\circ 40'$. The geometry of the molecule yields the following relation between the angle β and the angle Cl-C-Cl, defined as 2α ,

$$\cos 2\alpha = \frac{1}{2} (3 \cos^2 \beta - 1).$$

This analysis gave the following structural parameters for fluorotrichloromethane:

$$\text{C-Cl} = a = 1.76 \text{ \AA}$$

$$\text{C-F} = b = 1.33 \text{ \AA}$$

$$\text{Cl-C-Cl} = 2\alpha = 109^\circ 40'.$$

Electron diffraction data (17) for this molecule indicate C-Cl: 1.76 Å, C-F: 1.40 Å and Cl-C-Cl: 111.5° . There seems to be a discrepancy between the data for the C-F length; however, microwave data for C-F distances in other molecules (18) are as follows.

$\text{CF}_3\text{Cl}^{35}$:	1.32 Å
$\text{CF}_3\text{Br}^{79}$:	1.33 Å
CF_3I :	1.33 Å
CF_3H :	1.332 Å
CH_3F :	1.39 Å.

In addition, the Cl-C-Cl angle determined from the present investigation is approximately tetrahedral ($109^{\circ}28'$).

Nuclear Quadrupole Interaction Theory

The problem of three identical nuclei with quadrupole moments has been investigated by Bersohn (19) who obtained matrix elements for the interactions and by Mizushima and Ito (20) who used Bersohn's work to calculate the effect of quadrupole interaction on the $J = 0 \rightarrow 1$ rotational transition for a molecule with three identical nuclei with spins of 1, $3/2$, 2, and $5/2$. Also a theoretical investigation of the expected hyperfine structure of ND_3 was undertaken by Hadley (21). The first experimental work reported was that of Kojima et al (22) who applied the theoretical calculations of Mizushima and Ito to the $J = 0 \rightarrow 1$ rotational transition of bromoform (CHBr_3). The spectrum reported was proved later (23) to be of spurious origin. Wolfe (24) was the first to make a valid comparison of observed and calculated spectra for a molecule having three identical nuclei with quadrupole moments. Wolfe measured the $J = 2 \rightarrow 3$ rotational spectrum of the abundant symmetric top species of chloroform (CHCl_3^{35}) and calculated the spectrum by use of the procedure outlined by Bersohn. More recently Herrmann (25) made measurements on ND_3 (three nuclei of spin 1) and compared these with the theoretical work of Hadley.

The calculation of energies and intensities for three nuclei with quadrupole moments is laborious. For the case that Wolfe considered, the $J = 2 \rightarrow 3$ transition with spins of $3/2$, hundreds of transitions are possible between the two rotational levels. Because of the large number of overlapping lines it is difficult to find the result of superimposing

the components on the basis of a reasonable physical assumption of line shape. As pointed out by Wolfe, with his assumption of rectangular shapes, the positions of prominent features can be shifted somewhat from their true values, except in cases for which one component is considerably more intense than its neighbors. A complicating feature of the analysis results because centrifugal distortion allows different "centers" for the hyperfine patterns corresponding to each value of K . The quantum numbers $K = 0$, $K = 1$, and $K = 2$ are permissible for the $J = 2 \rightarrow 3$ transition. Wolfe investigated CHCl_3^{35} experimentally with relatively weak Stark fields in order to prevent second order Stark components from being sufficiently displaced to interfere with nuclear quadrupole hyperfine components. As a consequence, $K = 0$ components are not observed since these possess no first order Stark effect. Wolfe handled the problem of two values of K by shifting the relative positions of his calculated $K = 1$ and $K = 2$ patterns to obtain a best fit with his measured composite pattern. This technique provided a value for the quadrupole coupling constant and a value of the centrifugal distortion constant D_{JK} . Analysis of the $J = 1 \rightarrow 2$ transition for fluorotrichloromethane is even more difficult than the analysis of the chloroform spectrum. This is because the absorption coefficients of the lines are smaller and because the dipole moment of the molecule is so small that with usable electric fields the Stark components interfere with all but the strong lines. Analysis of the CFCl_3 spectrum required a theoretical calculation of the quadrupole splitting of the $J = 1 \rightarrow 2$ transition.

By means of the interactions of the nuclear quadrupole moments with the electric field gradient, the nuclear spin angular momenta, \underline{I}_i ,

$i = 1, 2, 3$, are coupled with the rotational angular momentum, \underline{J} , of the molecule to produce a resultant total angular momentum, $\underline{F} = \underline{J} + \underline{I}_1 + \underline{I}_2 + \underline{I}_3$. As a consequence, the rotational energy levels of the symmetric top are split into several components by the nuclear quadrupole interaction. The line splitting due to nuclear quadrupole interaction with three identical nuclei produces very complex hyperfine spectra, with complexity increasing rapidly with J .

The following discussion of nuclear quadrupole interaction follows Wolfe (15). His work on quadrupole interaction was specialized for the case of three identical nuclei of spin $3/2$; he used the general procedure outlined by Bersohn (19) for determining quadrupole fine structure of molecular rotational spectra. In addition, Wolfe predicted a spectrum for the $J = 2 \rightarrow 3$ rotational transition of chloroform.

In order to follow the method of Bersohn, which makes use of Racah algebra (26), in determining the perturbation energy E^1 due to the nuclear quadrupole interaction, the following unsymmetrical-appearing coupling scheme is employed in writing the nuclear-rotational wave functions:

$$\underline{I}_1 + \underline{I}_2 = \underline{L}, \quad L = I_1 + I_2, I_1 + I_2 - 1, \dots, I_1 - I_2$$

$$\underline{L} + \underline{I}_3 = \underline{I}, \quad I = L + I_3, L + I_3 - 1, \dots, L - I_3$$

$$\underline{I} + \underline{J} = \underline{F}, \quad F = I + J, I + J - 1, \dots, I - J.$$

The required nuclear-rotational wave functions are then

$$\langle I_1 I_2 I_3 L L J K F M | ;$$

they describe the states corresponding to the coupled nuclear spin angular momenta, \underline{I}_i , $i = 1, 2, 3$, and the rotational angular momentum, \underline{J} . These wave functions can be expressed as

$$\begin{aligned} \langle \underline{I}_1 \underline{I}_2 \underline{I}_3 \underline{L} \underline{I} \underline{J} \underline{K} \underline{F} \underline{M} | &= \sum_{m_1 m_2 m_3 m_J} (\underline{I}_1 \underline{I}_2 m_1 m_2 | \underline{L} m_L) (\underline{L} \underline{I}_3 m_L m_3 | \underline{I} m_I) \quad (2) \\ &\times (\underline{I} m_I m_J | \underline{F} \underline{M}) \psi(\underline{J} \underline{K} m_J) \varphi(\underline{I}_1 m_1) \varphi(\underline{I}_2 m_2) \varphi(\underline{I}_3 m_3). \end{aligned}$$

\underline{J} and \underline{I} were defined in this section; \underline{K} times $m_1, m_2, m_3, m_L, m_I, m_J$, and \underline{M} are the respective projections of $\underline{I}_1, \underline{I}_2, \underline{I}_3, \underline{L}, \underline{I}, \underline{J}$, and \underline{F} on a space-fixed Z direction ($m_1 = I_1, I_1 - 1, \dots, -I_1$; $m_L = J, J-1, \dots, -J$; etc.). $\psi(\underline{J} \underline{K} m_J)$ is the normalized rotational wave function for a rigid symmetric top, and $\varphi(\underline{I}_i m_i)$, $i = 1, 2, 3$, is the normalized nuclear wave function for the i^{th} chlorine nucleus in the state expressed in its argument. The quantities $(abcd|ef)$ are the vector-addition or Clebsch-Gordan coefficients, and are numerical functions of their arguments.

Perturbation theory specifies the E^1 as roots of the secular determinant

$$|H_{rr'}^1 - E^1 \delta(rr')| = 0,$$

where H^1 is the nuclear quadrupole interaction Hamiltonian, r specifies the state $\langle \underline{I}_1 \underline{I}_2 \underline{I}_3 \underline{L} \underline{I} \underline{J} \underline{K} \underline{F} \underline{M} |$, and r' the state $\langle \underline{I}_1 \underline{I}_2 \underline{I}_3 \underline{L}' \underline{I}' \underline{J}' \underline{K}' \underline{F}' \underline{M}' |$.

A classical consideration (19) of the electrostatic interaction between the nuclear quadrupoles and the electric field of the remainder of the molecule shows that H^1 may be written as the scalar product of two tensor operators of order two:

$$H^1 = \sum_{i=1}^n \left[Q(i) \cdot \nabla E(i) \right],$$

where n is the number of quadrupolar nuclei in the molecule. $Q(i)$ is called a quadrupole moment tensor and is a function of quantum number I_i ; $\nabla E(i)$ is the gradient of the electric field at the i^{th} nucleus due to the remainder of the molecule and is a function of quantum numbers J and K . Matrices for products such as are contained in the quadrupole interaction Hamiltonian were developed by Racah (26).

A partial diagonalization of the perturbation energy matrix can be made by taking into account the identity of the three quadrupolar nuclei. The group of permutations on three identical things has three irreducible representations: A_1 , A_2 , and E . A_1 is the one-by-one identity representation, A_2 is the one-by-one alternating representation and E is two-by-two. Since three identical nuclei are involved in this problem the nuclear states, $\langle LI|$, must belong to one or more of these representations, and the quadrupole Hamiltonian is invariant under their exchange and therefore commutes with the operators of the group. Hence it is possible to perform a transformation from the $\langle LI|$ nuclear representation to a representation $\langle SI|$, $S = A_1, A_2, E$, in which the energy matrix elements are diagonal in S . This follows because the S states are mutually orthogonal. When these transformations are employed, the non-vanishing matrix elements of H^1 diagonal in J and K become:

$$(SIJKF|H^1|SI'JKF) = (-1)^{F-J+\frac{1}{2}\lambda}(SII') G(JK) W(IJI'J;F2). \quad (3)$$

The $\lambda(\text{SII}')$ are related to Clebsch-Gordan coefficients used to express the wave functions as linear orthogonal combinations of the states S. Wolfe (Table 6 of reference 24) gives values of $\lambda(\text{SII}')$ required for analysis of molecules having three identical nuclei of spin 3/2. W is the Racah coefficient and is discussed in Appendix C. The coefficient $G(\text{JK})$ can be expressed as*

$$G(\text{JK}) = g(\text{JK}) eQV_{zz}, \quad (4)$$

where

$$g(\text{JK}) = \frac{3K^2 - J(J+1)}{2(J+1)} \left[\frac{5(2J+2)(2J+1)}{(2J+3)(2J)(2J-1)} \right]^{\frac{1}{2}}.$$

eQ is the electric quadrupole moment of the chlorine nucleus and V_{zz} is the second partial derivative of the electric potential at the chlorine nucleus (due to extranuclear charges), with respect to z , the symmetry axis of the molecule.

The total wave function for a molecule may be considered to be the product of three component wave functions:

$$\psi(\text{total}) = \psi(\text{electronic}) \psi(\text{vibrational}) \psi(\text{nuclear-rotational}).$$

For a molecule containing three identical nuclei the behavior of $\psi(\text{total})$ with respect to permutations of these three nuclei is then the product of the behaviors of the three component wave functions.

*The sign for $G(\text{JK})$ is incorrect in Equation 3 of reference 15; it is given correctly in Equation 17 of reference 24. Because of the error in Equation 3, the sign is also incorrect in Equation 6 of reference 15. These differences in sign were confirmed by personal communication with the author.

The great majority of molecules have totally symmetric, A_1 , ground electronic states. Fluorotrichloromethane is assumed to be no exception and consequently the symmetry property of $\psi(\text{electronic})$ does not enter into the determination of the behavior of $\psi(\text{total})$.

The following symmetry properties of the symmetric top wave functions are known (27). For the ground vibrational state, which is twofold because of the possibility of inversion of the molecule at its center of mass, $\psi(\text{vibrational})$ will be of species A_1 or A_2 . The rotational wave functions, $\psi(JK m_j)$, for $K = 1$ and $K = 2$ states are of species E. $K = 0$ will not be considered in the $J = 1 \rightarrow 2$ calculation because it does not give rise to first order Stark effect, and therefore was not observed.

According to Fermi-Dirac statistics obeyed by nuclei of half-integral spin, such as chlorine, $\psi(\text{total})$ must be antisymmetric in the three nuclei, that is, it must be of species A_2 . Hence $\psi(\text{nuclear-rotational})$ must be of species A_1 or A_2 , dependent upon whether the species of $\psi(\text{vibrational})$ is A_2 or A_1 . In other words, one of the following conditions must be satisfied for $\psi(\text{total})$ and $\psi(\text{electronic})$ to be A_2 and A_1 , respectively:

(1) If $\psi(\text{vibrational})$ is A_1 , $\psi(\text{nuclear-rotational})$ must be A_2 .

(2) If $\psi(\text{vibrational})$ is A_2 , $\psi(\text{nuclear-rotational})$ must be A_1 .

The nuclear-rotational wave functions involve products of the $\psi(JK m_j)$ and the nuclear wave functions. Since the $\psi(JK m_j)$ are of species E for the values of K under consideration, $K = 1$ and $K = 2$, the permissible nuclear states are of species E, otherwise the nuclear-rotational wave functions could not be of species A_1 or A_2 .

Relative intensities of the various hyperfine components of a given transition, $J \rightarrow J + 1$, are computed as the square of the matrix elements of the Z-component of the permanent electric dipole moment of the molecule, between the initial and final nuclear-rotational states involved in the transition. This computation yields (15) the following selection rules for the transitions $J \rightarrow J + 1$:

$$\begin{aligned}\Delta K &= 0 \\ S &\rightarrow S \\ \Delta F &= 0, \pm 1, \\ \Delta M &= 0.\end{aligned}$$

The intensities are summed over M because the hyperfine splitting is independent of this quantum number.

Wolfe determined an expression for the frequency shift of the most intense hyperfine component for any $J \rightarrow J + 1$ transition. This expression provides useful results from rotational-transition data for which the hyperfine spectrum has not been calculated. He found that the most intense component belongs to the set $K = 1$ and is specified by $F = J + \frac{7}{2} \rightarrow J + \frac{9}{2}$. Wolfe was able to obtain an expression in closed form because the energy matrices are always diagonal for these states and involve only the solution of one-by-one determinants. His expression, when modified to be in terms of the quadrupole coupling constant eQV_{zz} , is

$$\begin{aligned}\Delta\nu_Q &= \beta(J) eQV_{zz} \quad \text{where} & (5) \\ \beta &= -\frac{3}{4} \frac{(J+1)(J+2) + (4J+7)}{(2J+5)(2J+3)(J+2)(J+1)}.\end{aligned}$$

$\Delta\nu_Q$ is the frequency by which the most intense hyperfine component of the $J \rightarrow J + 1$ transition is shifted because of quadrupole interaction. The $J = 0 \rightarrow 1$ transition, having only $K = 0$ components, does not satisfy this relation.

Calculations for the $J = 1 \rightarrow 2$ Quadrupole Interaction Spectrum

Matrix elements $H'_{rr}/G(JK)$ were computed from Equation 3,

$$(SIJKF|H^1|SI'JKF)/G(JK) = (-1)^{F-J+\frac{1}{2}} \lambda(SII') W(IJI'J;F2),$$

and values of $\lambda(SII')$ obtained by Wolfe (24). The Racah coefficients were obtained by the methods discussed in Appendix C. The values of $\lambda(SII')$ and the matrix elements are listed in Table 8 (Appendix D). The three spin angular momenta are aligned parallel for $I = 9/2$; therefore the corresponding nuclear wave function is not permissible for a symmetric top molecule because it is symmetrical in the three nuclei (species A_1). The forms of the secular determinants for $J = 1$ and $J = 2$ are illustrated in Figure 2. The heavy outline is for $J = 1$; the $J = 2$ determinant includes elements enclosed by the dotted lines in addition to the elements applicable to $J = 1$. Diagonalization of the matrices involves the solution of one linear equation, 2 quadratic equations, and 2 cubic equations for a total of 11 roots for $J = 1$; one linear equation, 2 quadratic equations, one cubic equation and 2 quartic equations for a total of 16 roots for $J = 2$. Roots obtained in the present work for $J = 1$ are listed in Table 9 and those obtained by Wolfe for $J = 2$ are included in Table 10. These roots will be indicated by an index T.

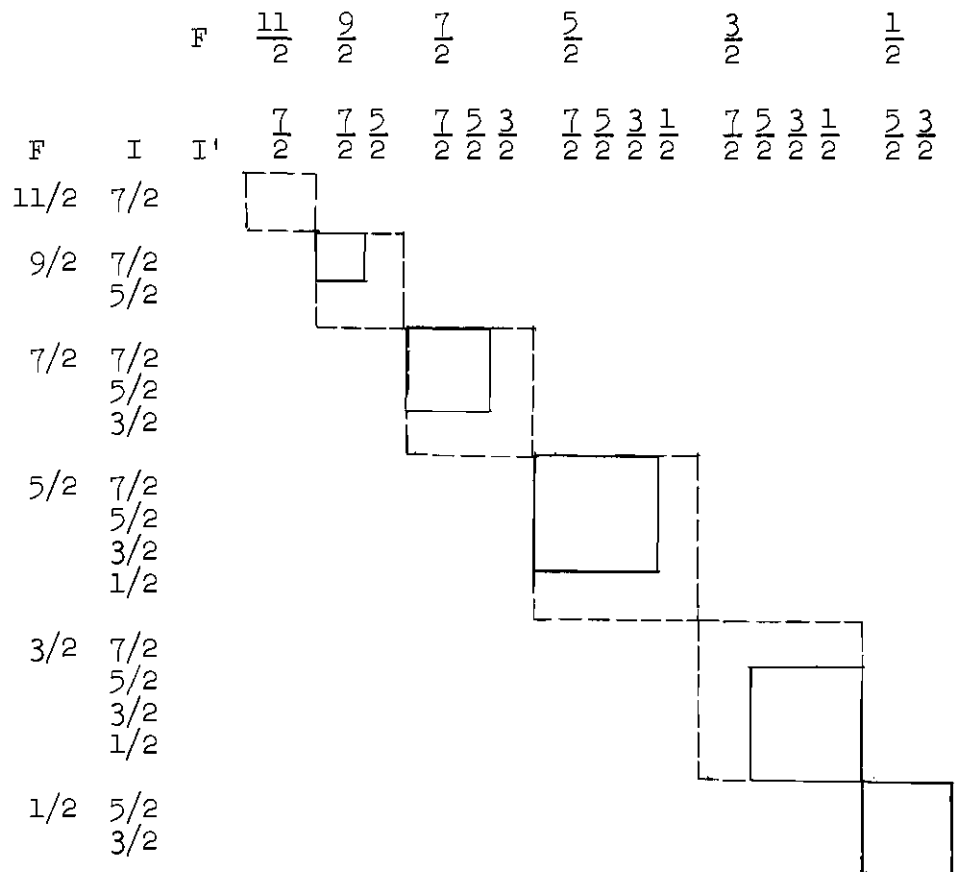


Figure 2. Graphical Description of Secular Determinants for $J = 1$ and for $J = 2$.

The nuclear quadrupole interaction energy is obtained by multiplying the above roots by $G(JK)$ defined in Equation 4. Equation 4 gives*

$$G(11) = 0.61237 eQV_{zz} \text{ and}$$

$$G(21) = -0.66815 eQV_{zz}.$$

The eigenvalues of the quadrupole interaction energy for the allowed nuclear states for $J = 1$ and 2 , $K = 1$ are given in Tables 9 and 10. Also included in these tables are approximate coefficients B_{TI} of the transformation matrices which accomplish the diagonalization. These coefficients are used in computing intensities.

A transition from a lower state, of energy

$$E_1(JKTF) = E_1^0(JK) + E_1^1(JKTF),$$

to an upper state, of energy

$$E_2(J+1KT'F') = E_2^0(J+1K) + E_2^1(J+1KT'F'),$$

is induced by radiation of frequency

$$f = (E_2 - E_1)/h = f_0 + \Delta\nu_Q,$$

where $f_0 = \left[E_2^0(J+1K) - E_1^0(JK) \right] / h$ is the unperturbed rotational frequency, $2B(J+1)$, and

*The sign given for $G(11)$ in Table 9 of reference 24 is incorrect; this was confirmed by personal communication with the author.

$$\Delta\nu_Q = \left[E_2^1(J+1KT'F') - E_1^1(JKTF) \right] / h$$

is the correction to f_0 caused by the nuclear quadrupole interaction perturbation. When eQV_{zz} is stated in units of frequency rather than energy, the factor h is omitted from the last expression:

$$\Delta\nu_Q = E_2^1(J+1KT'F') - E_1^1(JKTF). \quad (6)$$

According to Wolfe (24) the relative intensity, N , of a given $J = 1 \rightarrow 2$ transition for which $K = 1$ is

$$N = \left[\sum_I B_{TI} B_{T'I} R_I (FF') \right]^2 \quad (7)$$

where

$$R_I (FF') = \sqrt{(2F+1)(2F'+1)} W(1F2F';11).$$

Values of R_I for $J = 1 \rightarrow 2$, $K = 1$ are listed in Table 11. Most of the required Racah coefficients were calculated by hand using the techniques of Sharpe et al (see Appendix C); these are given in Table 12.

By means of the frequency relation, Equation 6, and the intensity expression, Equation 7, the data in Tables 9, 10, 11, and 12 give the frequencies and intensities of the $J = 1 \rightarrow 2$, $K = 1$, $\Delta F = 0 \pm 1$ transitions. There are a total of 99 hyperfine components but many of them are relatively weak. The increase in frequency, $\Delta\nu_Q$, in terms of eQV_{zz} and the relative intensity of these hyperfine components are listed in Table 13. These hyperfine components indicate two major prominences shifted in

frequency by approximately $-0.0607 eQV_{zz}$ and $+0.0643 eQV_{zz}$. Components contributing to these prominences are large compared to neighboring components. Therefore, a spectrum was calculated by using a half width for individual components, in terms of the experimentally determined value of eQV_{zz} , which gives line widths comparable to measured widths. Figure 3 shows the sums of intensities at intervals of $0.001 eQV_{zz}$. These intensities were summed by assuming that each component is Gaussian in shape and has a width between one-half intensity points of $0.015 eQV_{zz}$.

Experimental Results

Theoretical and experimental examinations were made for the hyperfine structure of the $J = 1 \rightarrow 2$ and $J = 2 \rightarrow 3$ transitions of $CFCl_3^{35}$. The frequency of the most intense prominence in the transitions $J = 3 \rightarrow 4$ through $J = 6 \rightarrow 7$ were experimentally determined. No previous microwave data have been reported for this molecule. Analysis of the $J = 1 \rightarrow 2$ spectrum provided a determination of the quadrupole coupling constant with respect to the molecular symmetry axis, eQV_{zz} , and the rotational constant B in terms of the centrifugal distortion constants D_{JK} and D_J . Based on the results of the $J = 1 \rightarrow 2$ investigation it was possible to interpret the very complex $J = 2 \rightarrow 3$ transition. This provided values for the distortion constants D_{JK} and D_J . Frequencies of the most intense prominences for the transitions $J = 3 \rightarrow 4$ through $J = 6 \rightarrow 7$ were used to verify the assignment for the most intense prominence of the $J = 2 \rightarrow 3$ spectrum.

In principle the analysis performed for the $J = 2 \rightarrow 3$ transition can be made without $J = 1 \rightarrow 2$ data. The following practical problems prohibit this:

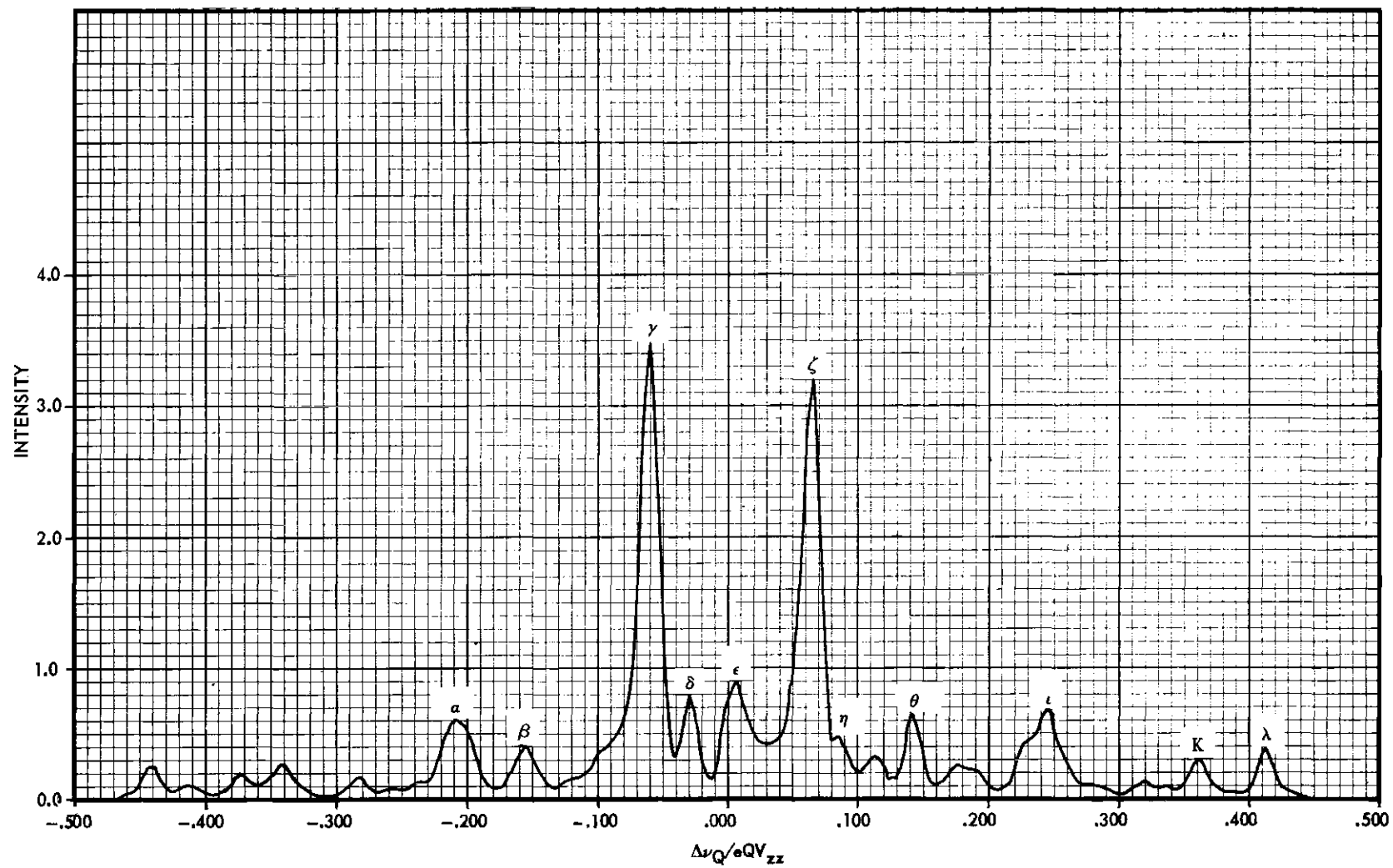


Figure 3. Predicted Quadrupole Interaction Spectrum for $J = 1 \rightarrow 2$ Transition.

(1) the lines are so weak that only the stronger prominences of the $J = 2 \rightarrow 3$ hyperfine structure could be identified, and

(2) the molecular dipole moment is so small that the maximum usable Stark field (limited by electrical breakdown of the waveguide cell) is not sufficiently large to remove the Stark components from the $J = 2 \rightarrow 3$ hyperfine structure.

Analysis of the $J = 1 \rightarrow 2$ data provided a determination of the quadrupole coupling constant eQV_{zz} . Knowledge of this constant permitted recognition of the major prominences in the $J = 2 \rightarrow 3$ spectrum. With this information it was possible to determine a value for the centrifugal distortion constant D_{JK} from the $J = 2 \rightarrow 3$ spectrum.

The Stark effect in symmetric top molecules with nuclear quadrupole coupling has been treated by Low and Townes (28). Their work yields displacement frequencies of

$$2\mu E m_J K / hJ(J+1)(J+2) \quad (8)$$

for the $J \rightarrow J + 1$ transition, spread slightly by the quadrupole interactions. The maximum usable Stark voltage is limited by electrical breakdown of the gas in the cell. Lowering the pressure will allow the use of higher Stark voltages but will reduce the intensity of absorption lines. Stark fields ranging between 160 v/cm and 640 v/cm were used in studying the $J = 1 \rightarrow 2$ and $J = 2 \rightarrow 3$ spectra. For a dipole moment of 0.45 debye (29) for CFCl_3 and a Stark field of 160 v/cm, the above expression gives ± 12 mc for the minimum $J = 1 \rightarrow 2$ displacement frequency. No Stark interference was observed for the $J = 1 \rightarrow 2$ transition. For the $J = 2 \rightarrow 3$ spectrum and the range of Stark fields used, Stark components

are expected between ± 3 mc and ± 12 mc, ± 6 mc and ± 24 mc, and ± 12 mc and ± 48 mc. The three frequency ranges correspond to $m_J = 1, 2$ for $K = 2$ and $m_J = 1$ for $K = 1$. For this reason, only data from the strong $J = 2 \rightarrow 3$ prominences at the center of the hyperfine spectrum could be used with any assurance to investigate the molecule.

$J = 1 \rightarrow 2$ Spectrum.--In an attempt to verify the predicted hyperfine structure and to evaluate the quadrupole coupling constant, eQV_{zz} , the $J = 1 \rightarrow 2$ transition of the most abundant symmetric top species of fluorotrichloromethane was examined repeatedly, under various conditions of pressure and Stark field. Typical results are shown in the recorder tracings of Figures 4 and 5.

Two relatively strong lines which are almost equal in intensity and several smaller lines were observed. Based on about thirty measurements for each line taken at pressures of 30μ or less, the two stronger lines were observed at 9859.30 ± 0.04 mc and 9863.96 ± 0.05 mc. The indicated errors are probable errors under the assumption that the errors are normally distributed about the mean frequencies.

From Table 13 it is seen that the quadrupole interaction produces a shift in frequency of $-0.06071 eQV_{zz}$ in the most intense line and $+0.06429 eQV_{zz}$ in the other strong line. Therefore the frequency difference of these lines is $0.1250 eQV_{zz}$. The difference in measured frequencies is 4.66 ± 0.06 mc. This gives

$$eQV_{zz} = 37.3 \pm 0.5 \text{ mc.}$$

Assuming that the $K = 0$ transition is not observable, the only value of K which is permissible is $K = 1$. The spectrum in absence of the quadrupole interaction would then be a single line frequency f_1 , where

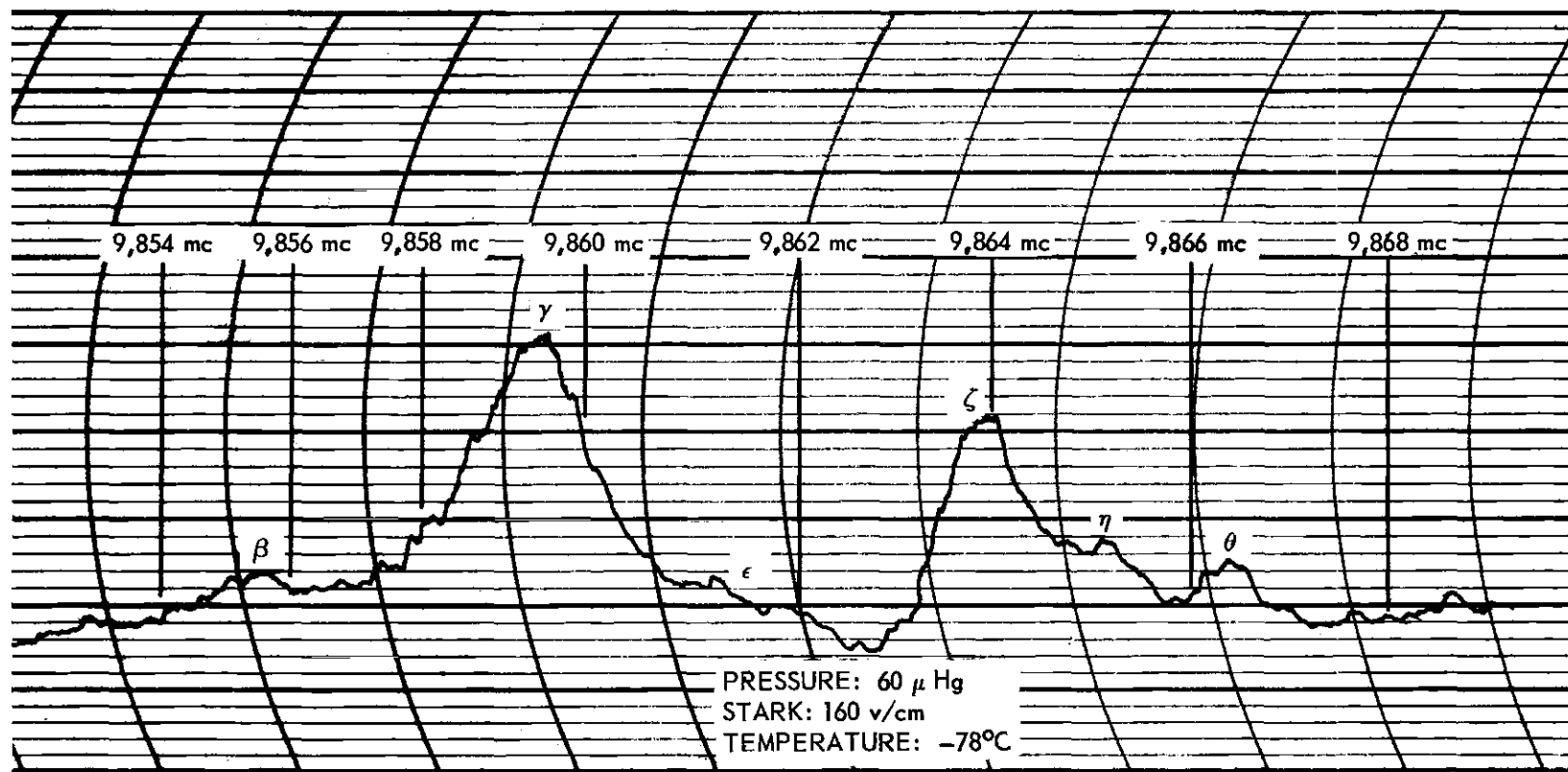


Figure 4. $J = 1 \rightarrow 2$ Transition in CFCl_3^{35} at 60 μ Pressure.

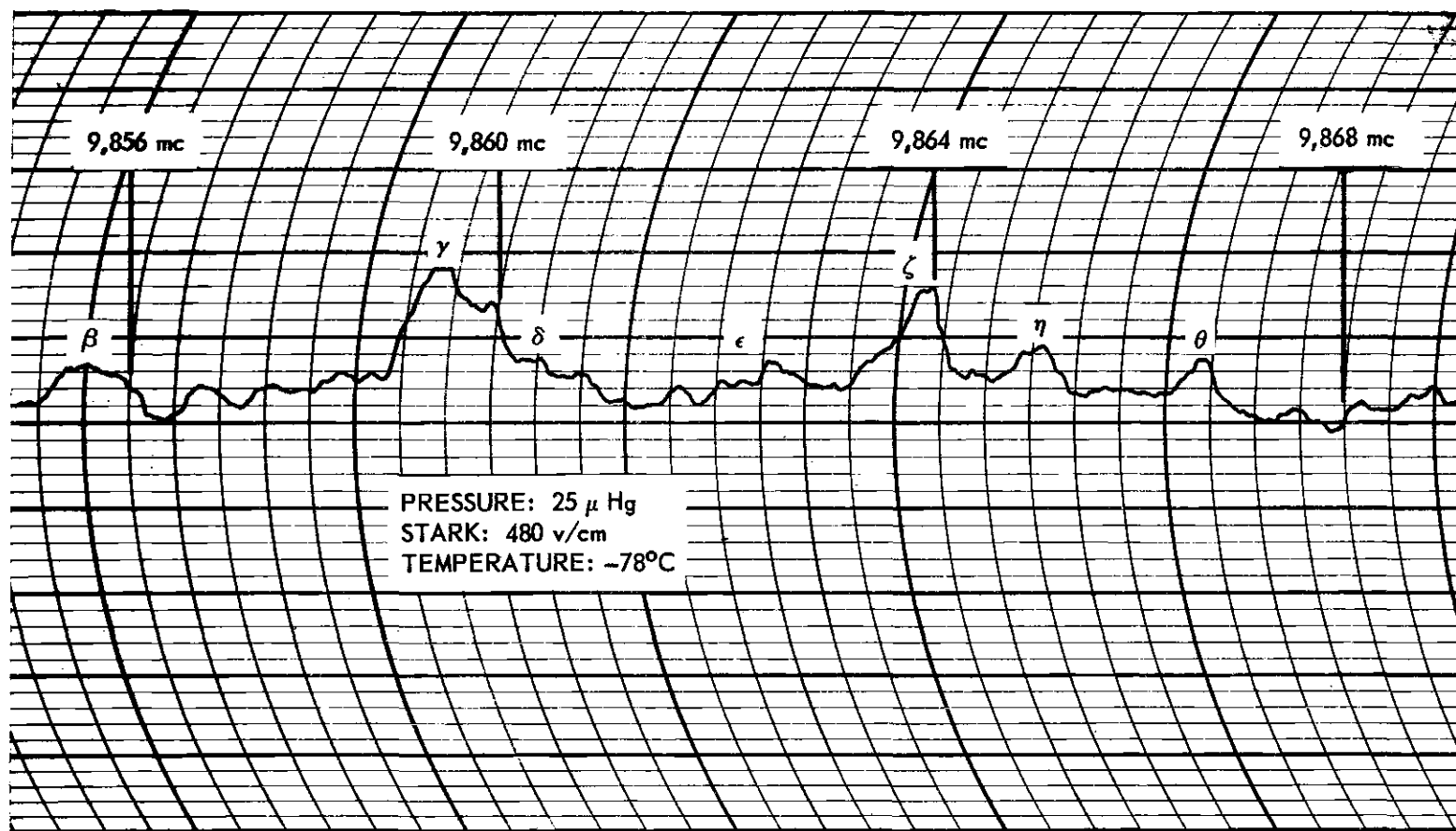


Figure 5. $J = 1 \rightarrow 2$ Transition in CFCl_3^{35} at 25 μ Pressure.

$$f_1 = f - \Delta\nu_Q = (9859.30 \pm 0.04) - (-0.06071)(37.3 \pm 0.5) \quad (9)$$

$$= 9861.56 \pm 0.05 \text{ mc.}$$

Use of Equation 1 and Equation 8 gives

$$B-D_{JK}-8D_J = 2465.39 \pm 0.01 \text{ mc.} \quad (10)$$

Frequency f_1 of Equation 9 and eQV_{zz} of 37.3 ± 0.5 mc were used to calculate frequencies for major prominences of Figure 3. Comparisons between the calculated and observed frequencies are given in Table 3. The relative intensities given in this table for prominences consisting of more than one line were taken from Table 13, Appendix D. Prominences marked weak were not observed on all recordings; there may be other weak prominences of comparable intensity not recorded in Table 3.

The absorption of a spectral line at its maximum is generally expressed for a temperature of 300°K. For symmetric top molecules and a line width of 25/mc mm pressure, this absorption may be expressed (30) as

$$\gamma = 4.94 \times 10^{-22} \sqrt{C} \mu^2 \nu^3 \left[1 - \frac{K^2}{(J+1)^2} \right] \text{ cm}^{-1}. \quad (11)$$

In this expression

μ = dipole moment in debye units (10^{-18} esu/cm)

ν = the frequency in megacycles

C = the rotational constant about the figure axis in megacycles
 $= 10^{-6} h/8\pi^2 I_C$.

Table 3. Observed and Calculated Features of the J = 1→2
Hyperfine Spectrum

Designation	Observation		Calculation		
	Frequency mc	Intensity cm ⁻¹	Frequency mc	Relative Intensity	Intensity cm ⁻¹
α	9853.68 ± 0.08	Medium	$\left\{ \begin{array}{l} 9853.47 \pm 0.09 \\ 9853.59 \pm 0.09 \\ 9853.95 \pm 0.09 \\ 9854.08 \pm 0.09 \\ 9854.11 \pm 0.09 \end{array} \right\}$	$\left\{ \begin{array}{l} 0.14 \\ 0.37 \\ 0.14 \\ 0.12 \\ 0.19 \end{array} \right\}$	7.7 × 10 ⁻¹¹
β	9855.60 ± 0.20	Weak	$\left\{ \begin{array}{l} 9855.34 \pm 0.06 \\ 9855.76 \pm 0.06 \end{array} \right\}$	$\left\{ \begin{array}{l} 0.12 \\ 0.35 \end{array} \right\}$	5.0 × 10 ⁻¹¹
γ	9859.30 ± 0.04	3.3 × 10 ⁻¹⁰ (Strong)	fitted		4.5 × 10 ⁻¹⁰
δ	9860.60 ± 0.10	Medium	9860.48 ± 0.04		9.5 × 10 ⁻¹¹
ε	9861.80 ± 0.30	Weak	$\left\{ \begin{array}{l} 9861.56 \pm 0.05 \\ 9861.69 \pm 0.05 \\ 9861.72 \pm 0.05 \\ 9861.75 \pm 0.05 \end{array} \right\}$	$\left\{ \begin{array}{l} 0.15 \\ 0.32 \\ 0.50 \\ 0.01 \end{array} \right\}$	1.0 × 10 ⁻¹⁰
ζ	9863.96 ± 0.05	3.0 × 10 ⁻¹⁰ (Strong)	fitted		4.1 × 10 ⁻¹⁰
η	9865.00 ± 0.20	Weak	9864.78 ± 0.05		5.9 × 10 ⁻¹¹
θ	9866.69 ± 0.11	7.4 × 10 ⁻¹¹ (Medium)	9866.85 ± 0.07		8.6 × 10 ⁻¹¹
ι	9870.50 ± 0.20	Medium	9870.62 ± 0.10		8.6 × 10 ⁻¹¹
κ	9875.00 ± 0.25	Weak	9874.96 ± 0.16		3.9 × 10 ⁻¹¹
λ	9877.00 ± 0.25	Weak	9876.94 ± 0.18		5.0 × 10 ⁻¹¹

This formula holds for one particular value of K. In case K is not zero, transitions corresponding to +K and -K are always superimposed, thus the expression must be doubled to account for this effect in the $J = 1 \rightarrow 2$ transition. The rotational constant C was calculated for the molecular dimensions obtained in the present research, and was found to be 1747 mc. For a ν of 9860 mc, μ of 0.45 debye (29), J and K of unity, Equation 11 gives

$$\gamma = 6.0 \times 10^{-9} \text{ cm}^{-1}.$$

The intensities when calculated as above must be modified to take into account the following effects:

1. depletion due to less than 100 per cent abundance of the isotopes giving rise to the absorption, and
2. splitting of the line into hyperfine components.

From the description of fluorotrichloromethane we know that 27/64 of the molecules are of species CFCl_3^{35} . Therefore if no splitting of the line into hyperfine components occurred, the maximum absorption coefficient would be

$$\gamma = 2.53 \times 10^{-9} \text{ cm}^{-1}.$$

The multiplicative factor by which the most intense line is reduced because of quadrupole interaction was determined from Table 13. This factor was obtained by dividing the sum of intensities of components contributing to the major prominence, γ in Figure 3, by the sum of all intensities in Table 13. The resultant calculated intensity for room temperature of the most intense line is

$$\gamma = 4.5 \times 10^{-10} \text{cm}^{-1}.$$

Other calculated intensities were obtained from the intensity of γ by using the relative intensities indicated by Figure 3; these are included in Table 3.

The absorption coefficients of three relatively strong lines (γ , ζ , θ) were also determined by comparing the line strengths with the measured noise level of the spectrograph, expressed in terms of absorption coefficient. This comparison, which was made for the gas at dry-ice temperature, indicated absorption coefficients of $9 \times 10^{-10} \text{cm}^{-1}$, 8×10^{-10} , and $2 \times 10^{-10} \text{cm}^{-1}$. Line intensity for a symmetric top molecule varies (27) with temperature as $T^{5/2}$. Results of the absorption coefficient measurements expressed for room temperature are given in Table 3. The agreement between calculated and measured absorption coefficients is good in view of errors which necessarily exist for sensitivity measurements of the type required for this problem.

J = 2→3 Spectrum.--Problems associated with analysis of the J = 2→3 rotational spectrum are reduced significantly if only data on the more intense lines are required. Because of this, the centrifugal distortion constant D_{JK} was evaluated through a determination of the difference in the frequencies of the most intense line for K = 1 and the most intense line for K = 2 in the J = 2→3 spectrum. Calculations of the predicted frequencies for this transition are based on the work of Wolfe.

The data in Tables 14 and 15 give the frequencies and intensities for the J = 2→3, K = 1 and K = 2 transitions, respectively. These tables were computed from the calculations of Wolfe (31) by simply mul-

tipling his data by -2.8688 , the constant which converts frequencies in terms of quadrupole coupling constant with respect to the bond axis to frequencies in terms of quadrupole coupling constant with respect to the molecular symmetry axis, eQV_{zz} . Figures 6 and 7 show the sums of the intensities in Tables 14 and 15 at intervals of $0.005 eQV_{zz}$, each sum containing all components which lie within $0.005 eQV_{zz}$ of its center. The summation of components within $0.005 eQV_{zz}$ was required to obtain the correspondence between measured and predicted hyperfine spectra shown in Figure 10.

Figure 8 is typical of recordings made using pressures of 30μ or less. Equipment sensitivity was such that 10μ was the lowest pressure for which prominences C, E, and F could be seen in a recording. Results of repeatedly measuring frequencies of the major prominences are given in Table 4. Figure 9 illustrates a typical spectrum measured with pressures between 60μ and 150μ . The frequency of the second-strongest prominence, C of Figure 9, corresponds to that of the strongest prominence, C, for the low pressure case illustrated in Figure 8. The largest prominence (E,F) of Figure 9 corresponds to a frequency intermediate to prominences E and F of Figure 8, indicating that the strongest high-pressure prominence contains components E and F. A comparison of Figure 8 with Figures 6 and 7 suggests that the largest component, C, corresponds to the strongest component (designated as e in Figure 6 and Table 14) of the predicted spectrum for $K = 1$.

From data similar to Figure 9, it was seen that the smallest Stark displacement is 2.9 mc for a nominal field of 180 volts/cm . These data

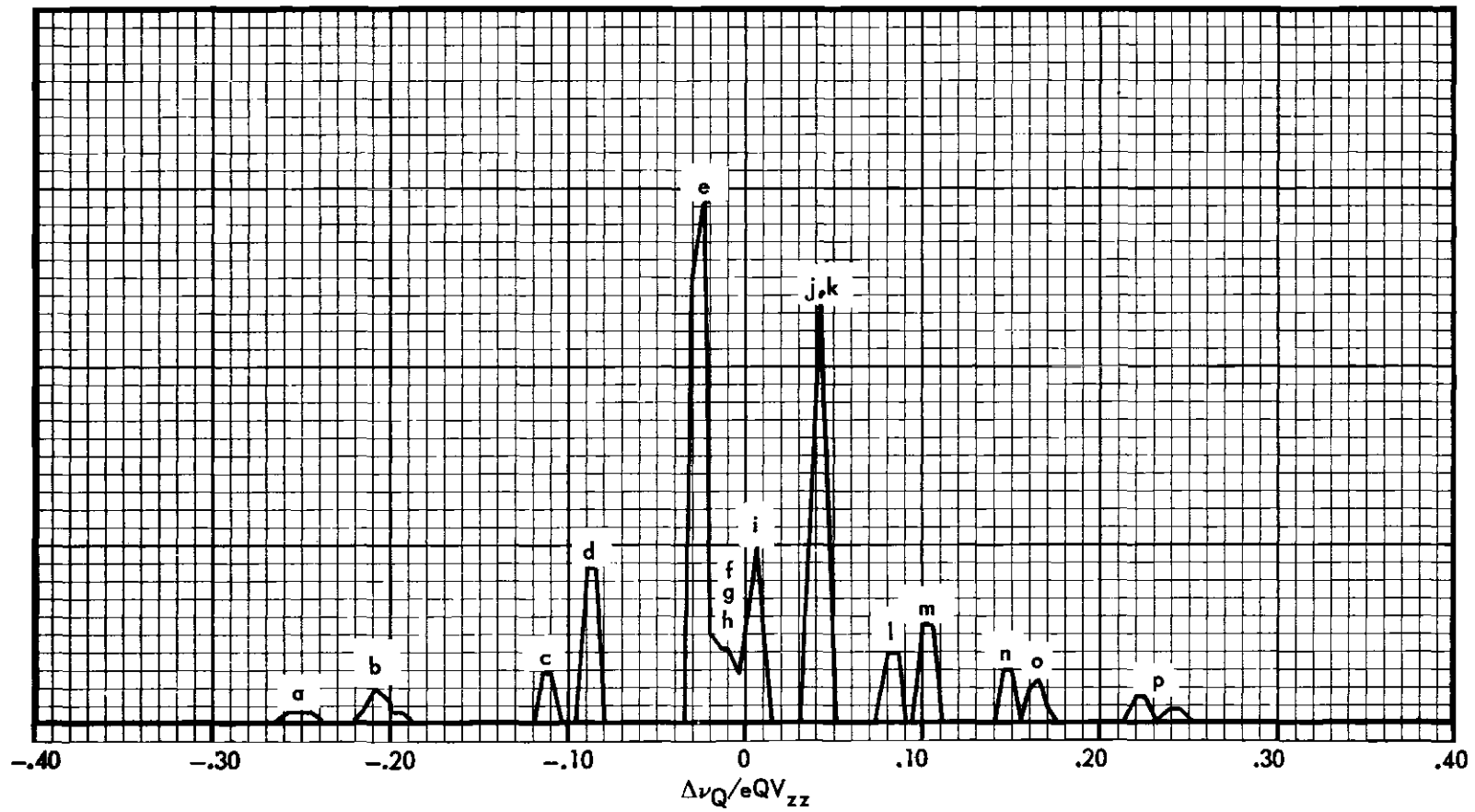


Figure 6. Predicted Hyperfine Pattern, $J = 2 \rightarrow 3$, $K = 1$.

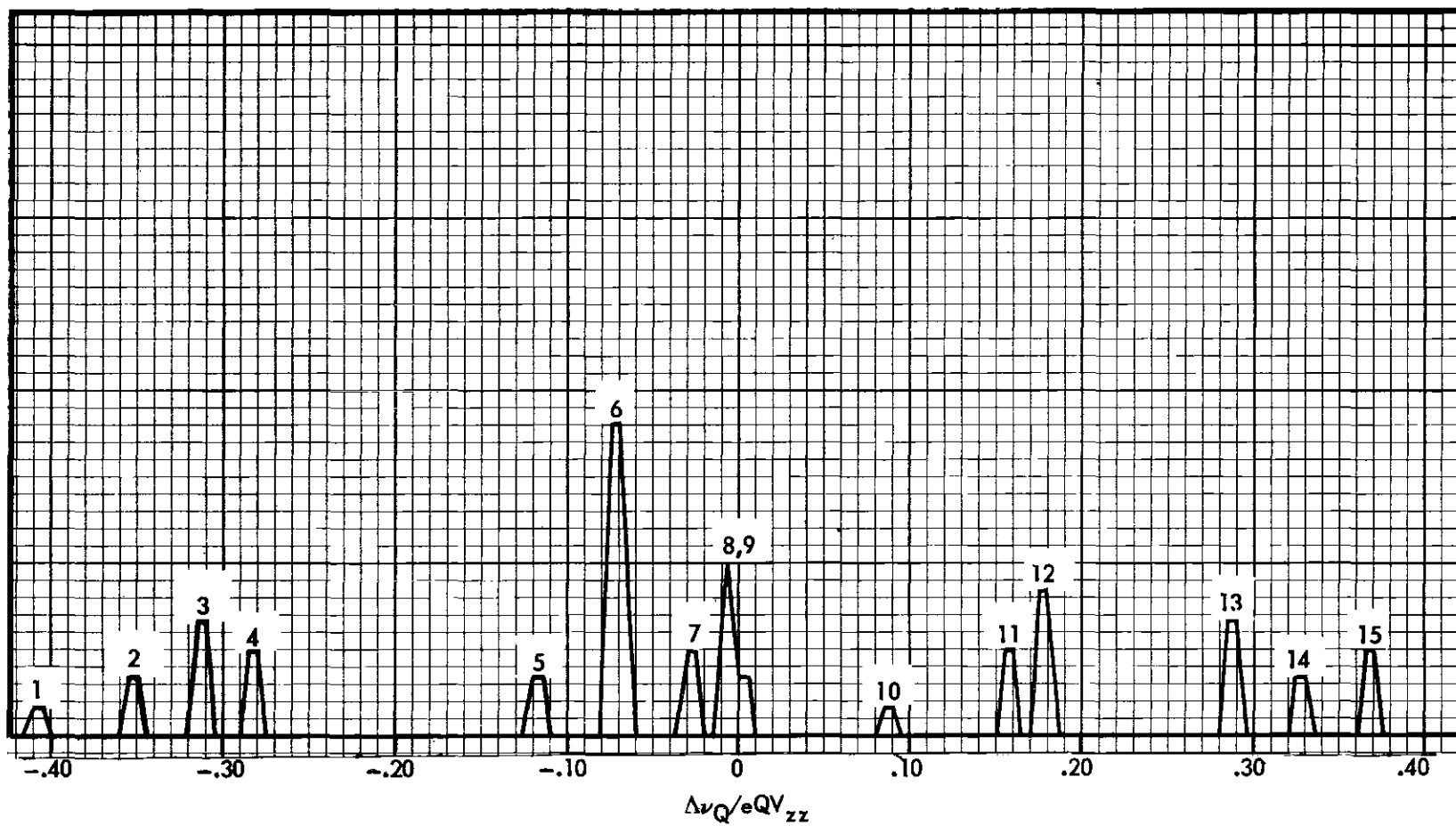


Figure 7. Predicted Hyperfine Pattern, $J = 2 \rightarrow 3$, $K = 2$.

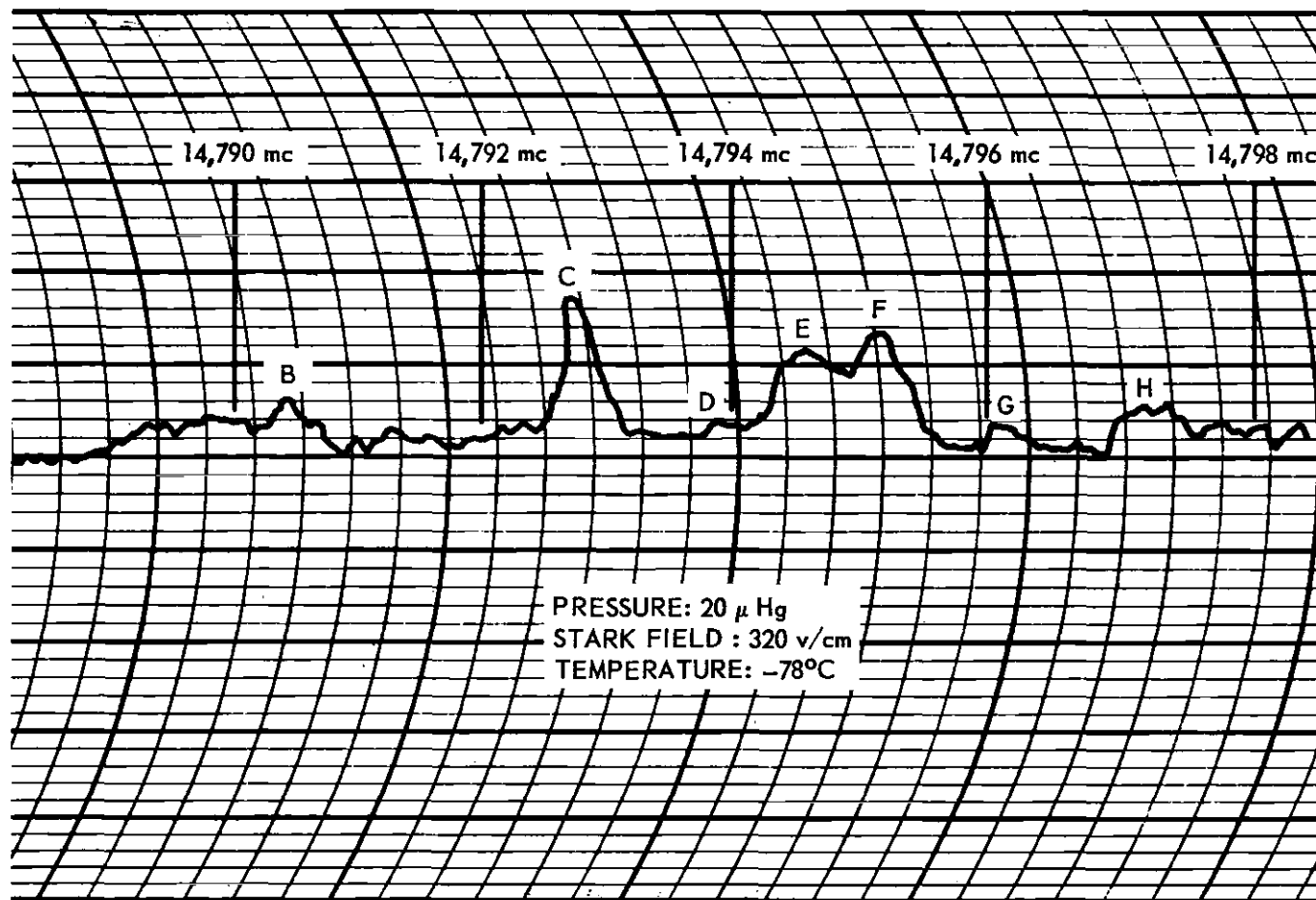


Figure 8. $J = 2 \rightarrow 3$ Transition in CFCl_3^{35} at 20 μ Pressure.

Table 4. Observed and Calculated Features of the J = 2→3
Hyperfine Spectrum

Observation				Calculation		
Designation	Frequency mc	Intensity	K	Designation	Frequency mc	Intensity
	unobserved		2	1	14,782.08 ± 0.19	19
A	14,784.75 ± 0.10	M*	2	2	14,784.25 ± 0.16	39
			1	a	14,784.37 ± 0.13	9
			2	3	14,785.64 ± 0.14	78
			1	b	14,786.02 ± 0.11	26
	unobserved		2	4	14,786.73 ± 0.14	58
B	14,790.46 ± 0.08	W	1	c	14,789.59 ± 0.07	33
			1	d	14,790.52 ± 0.07	99
C	14,792.80 ± 0.06	S	1	e	fitted	288
			2	5	14,792.94 ± 0.07	39
			1	f	14,793.00 ± 0.06	59
			1	g	14,793.24 ± 0.06	46
D	14,793.92 ± 0.08	W	1	h	14,793.59 ± 0.06	35
			1	i	14,793.95 ± 0.06	118
E	14,794.66 ± 0.08	S	2	6	fitted	214
F	14,795.26 ± 0.08	S	1	j	14,795.14 ± 0.07	195
			1	k	14,795.46 ± 0.07	83
G	14,796.25 ± 0.10	W	2	7	14,796.29 ± 0.08	58

*Intensities are S, strong; M, medium; W, weak.

Table 4. Observed and Calculated Features of the $J = 2 \rightarrow 3$ Hyperfine Spectrum (Continued)

Observation				Calculation		
Designation	Frequency mc	Intensity	K	Designation	Frequency mc	Intensity
H	$14,797.12 \pm 0.10$	M	1	ℓ	$14,796.84 \pm 0.08$	46
			2	8	$14,797.02 \pm 0.09$	78
			2	9	$14,797.32 \pm 0.09$	39
			1	m	$14,797.77 \pm 0.09$	65
I	$14,799.50 \pm 0.30$	W	1	n	$14,799.28 \pm 0.11$	34
			1	o	$14,799.85 \pm 0.11$	31
			2	10	$14,800.58 \pm 0.11$	19
			1	p	$14,802.38 \pm 0.14$	29
J	$14,803.40 \pm 0.30$	W	2	11	$14,803.18 \pm 0.14$	58
			2	12	$14,803.98 \pm 0.15$	97
			2	13	$14,807.98 \pm 0.20$	78
			2	14	$14,809.45 \pm 0.21$	39
			2	15	$14,811.09 \pm 0.23$	58
			unobserved			

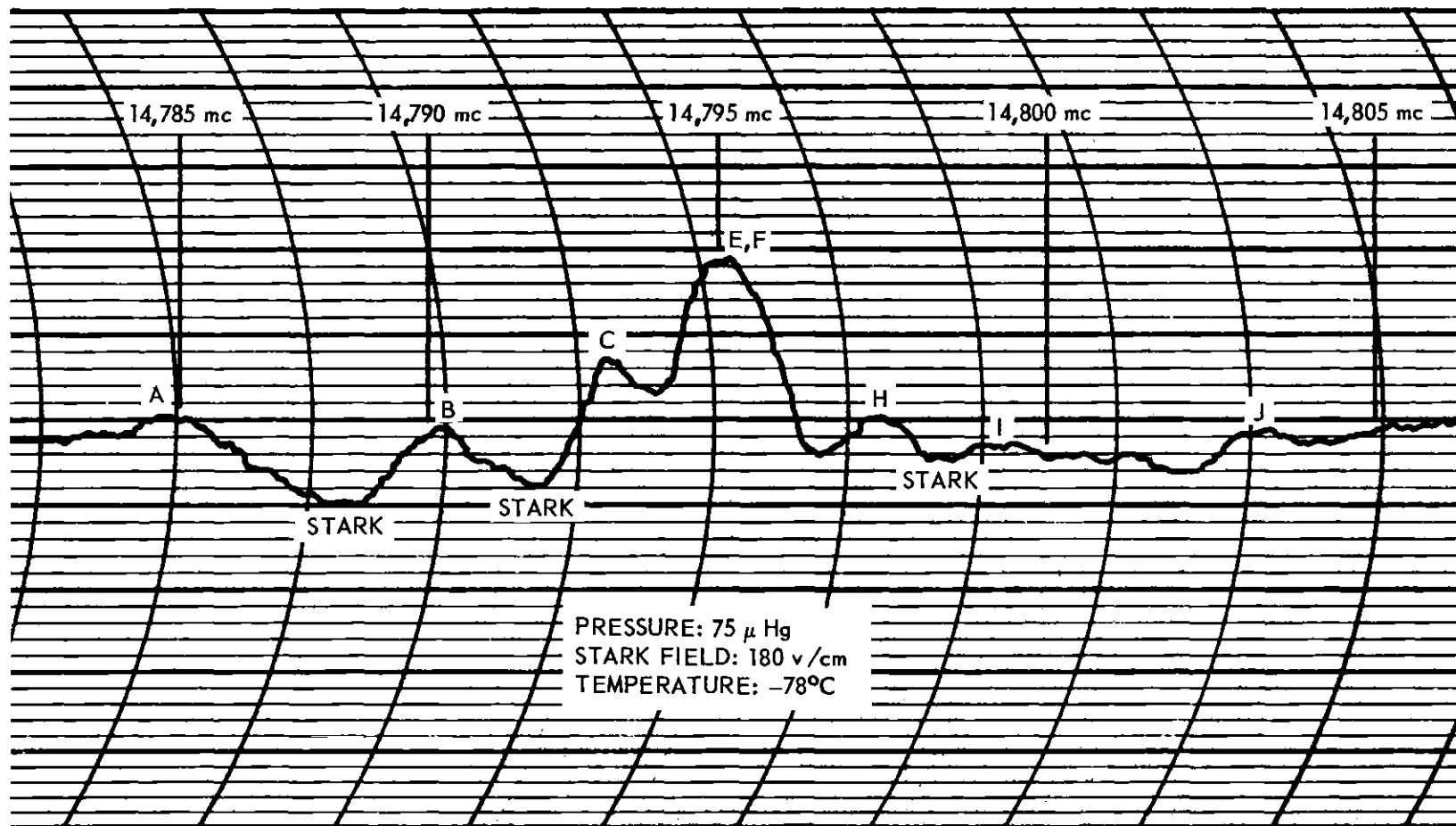


Figure 9. $J = 2 \rightarrow 3$ Transition in CFCl_2^{35} at 75 μ Pressure.

and Equation 8 yield a value of dipole moment which gives approximate agreement with the value of 0.45 debye obtained by low frequency measurements (28).

The following calculation was used to determine the approximate frequency of the most intense $J = 2 \rightarrow 3$ component based on the $J = 1 \rightarrow 2$ data and the predicted $J = 2 \rightarrow 3$ hyperfine spectrum. Use of Equation 1 evaluated for $J = 2, K = 1$ yields

$$f = 6(B - D_{JK}) - 108D_J + \Delta v_Q = 6(B - D_{JK} - 8D_J) - 60D_J + \Delta v_Q. \quad (12)$$

Equation 5 for $J = 2$ and eQV_{zz} equal to 37.3 ± 0.5 mc gives

$$\Delta v_Q = -1.00 \pm 0.01 \text{ mc.} \quad (13)$$

The result of substituting Equations 10 and 13 into Equation 12 is

$$f = 14,791.34 - 60D_J \pm 0.06.$$

Because it appeared that no major prominence* had a frequency corresponding to this expected frequency (based on the $J = 1 \rightarrow 2$ spectrum), considerable effort was devoted to measuring spectra corresponding to larger values of J . According to the work described in the section which follows, prominence C in Figure 8 is the only line that can correspond to the strongest line in the $K = 1$ spectrum. On the basis of the above, prominence E must indeed correspond to component e of the predicted spectrum because prominence C is (a) the strongest component observed at low

*A negative value of D_J is required to obtain agreement in frequency; previous investigations for other molecules have yielded only positive values (32).

pressures, and (b) the only observed prominence having a frequency compatible with measured components of other rotational spectra.

On the basis of the relative intensities of major components in the predicted spectra, prominence E is expected to correspond to the most intense component in the $K = 2$ spectrum (designated as b) and prominence F is expected to correspond to the second-most intense component in the $K = 1$ spectrum (designated as j, k). At the lower pressures, the frequency of the peak of (j, k) is due almost entirely to component j of Table 14. If this assignment of components is correct, the frequency of prominence F, according to Table 4, will exceed that of prominence C by $0.0626 eQV_{zz}$. By using 37.3 ± 0.5 mc for eQV_{zz} (obtained from the $J = 1 \rightarrow 2$ spectrum) and $14,792.80 \pm 0.06$ mc for C, it is then predicted that the component corresponding to the second-most intense component of the $K = 1$ spectrum will be located at $14,795.14 \pm 0.07$ mc. This must correspond to the observed feature F at $14,795.26 \pm 0.08$ mc.

The assumption, based on relative intensities, that E corresponds to the most intense component of the $K = 2$ spectrum can be tested by comparing a predicted spectrum, obtained by adding the two predicted spectra, with the observed composite spectrum.

The amount that the $K = 2$ spectrum must be shifted with respect to the $K = 1$ spectrum, because of centrifugal distortion, is calculated below. For the most intense component in the $K = 1$ spectrum

$$6B - 6D_{JK} - 108D_J - 0.02679 (37.3 \pm 0.5) = 14,792.80 \pm 0.06,$$

and for the most intense component in the $K = 2$ spectrum

$$6B - 24D_{JK} - 108D_J - 0.07143 (37.3 \pm 0.5) = 14,794.66 \pm 0.08.$$

A combination of these equations gives

$$D_{JK} = -196 \pm 6 \text{ kc.}$$

Figure 10 shows a comparison of the measured prominences with the predicted prominences; the general agreement in line structure indicates a valid assignment of components. Table 4 contains calculated frequencies for all components listed in Tables 14 and 15. These calculated frequencies are compared with the frequencies corresponding to the measured prominences. Although several of the weaker components were not identified, a sufficient number of other prominences were identified to verify that the value of eQV_{zz} obtained for the $J = 1 \rightarrow 2$, $K = 1$ spectrum is valid for the $J = 2 \rightarrow 3$, $K = 1$ and 2 spectra.

The absorption coefficient of the most intense component of the $J = 2 \rightarrow 3$ spectrum was calculated by the same method used for the most intense component of the $J = 1 \rightarrow 2$ spectrum. Equation 11 and data from Table 14 provide an absorption coefficient of $2.5 \times 10^{-9} \text{ cm}^{-1}$; the corresponding coefficient for the $J = 1 \rightarrow 2$ transition is $4.5 \times 10^{-10} \text{ cm}^{-1}$. The increased absorption coefficient for the $J = 2 \rightarrow 3$ over the $J = 1 \rightarrow 2$ value is offset by a lower spectrometer sensitivity. The sensitivity is lower because the LN78B crystal detectors used for the $J = 2 \rightarrow 3$ region are less efficient than the LN23E crystals used for the $J = 1 \rightarrow 2$ region.

Other Rotational Transitions.—Measurements were made for the frequencies of the largest resolvable prominence at pressures of about 25μ for each of the rotational transitions $J = 3 \rightarrow 4$ to $J = 6 \rightarrow 7$, inclusive. The

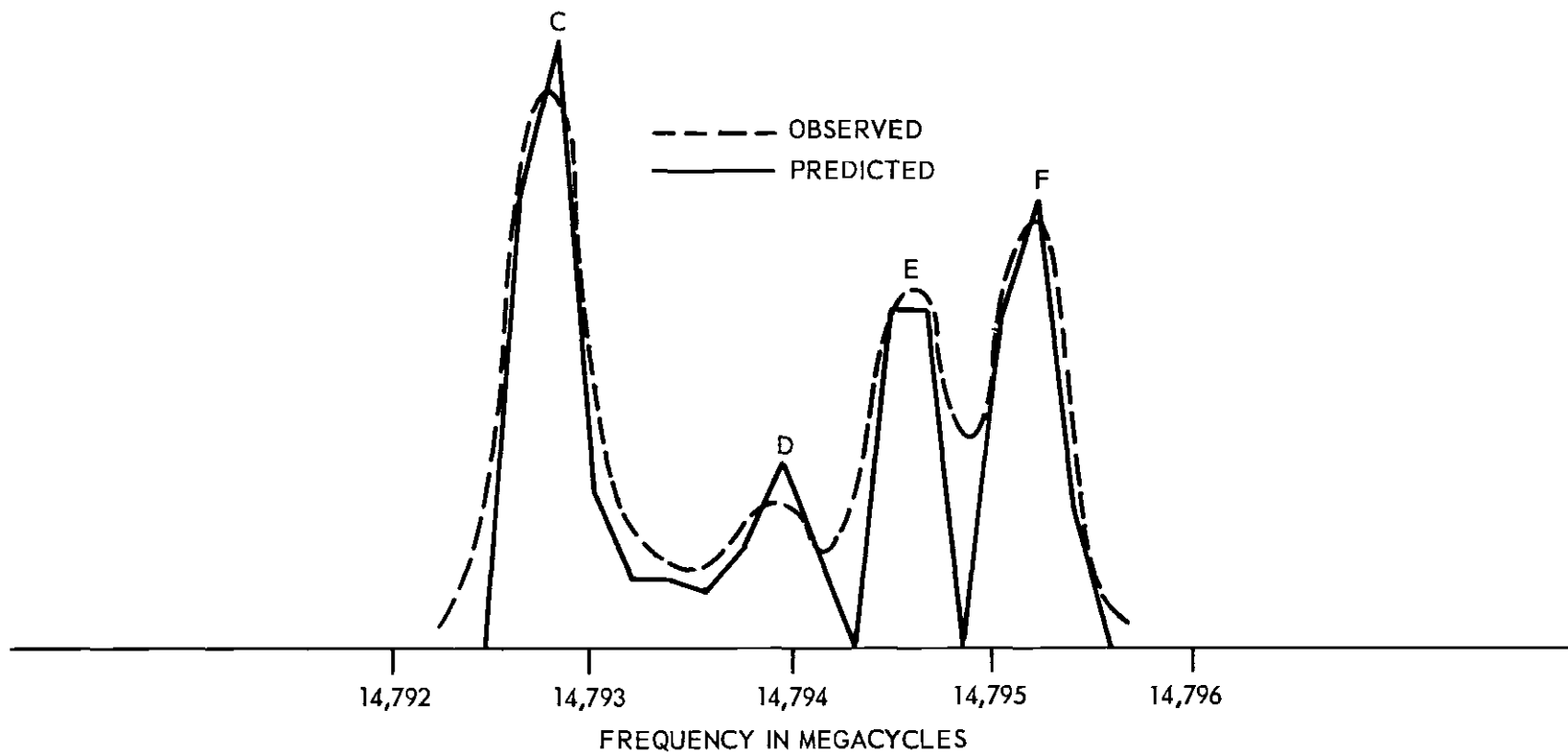


Figure 10. Observed and Calculated Features of the $J = 2 \rightarrow 3$ Transition in CFCl_3^{35} .

measurements were used to assist in the assignment of the major prominences in the $J = 2 \rightarrow 3$ hyperfine spectrum. The results were analyzed with Equation 5,

$$\Delta\nu_Q = \beta(J)eQV_{zz},$$

where

$$\beta(J) = -\frac{3}{4} \left[\frac{(J+1)(J+2)+(4J+7)}{(2J+5)(2J+3)(J+2)(J+1)} \right].$$

$\Delta\nu_Q$ is the frequency by which the largest individual line is shifted as a result of quadrupole interaction. Results of the measurements and calculations, including those for the $J = 1 \rightarrow 2$ and $J = 2 \rightarrow 3$ spectra, are given in Table 5. Because the strongest component is expected to correspond to $K = 1$, Equation 1 may be expressed as

$$\frac{f - \Delta\nu_Q}{2(J+1)} = (B - D_{JK}) - 2D_J(J+1)^2. \quad (14)$$

The values in the right-hand column for the $J = 1 \rightarrow 2$ and $J = 3 \rightarrow 4$ transitions assist in assigning the frequency of the largest measured prominence in the $J = 2 \rightarrow 3$ hyperfine spectrum at low pressures to the frequency corresponding to the largest individual line in the predicted spectrum. The frequency of this $J = 2 \rightarrow 3$ component is expected to occur within the limits of frequencies corresponding to the values of $(f - \Delta\nu_Q)/2(J+1)$ for the $J = 1 \rightarrow 2$ and $J = 3 \rightarrow 4$ spectra. Based on Table 5, it should lie between 14,791.3 mc and 14,793.3 mc; prominence C (Table 4) is the only observable prominence within these limits.

Table 5. Frequencies of the Strongest Line in Various Spectra

Transition	Measured Frequency, f , of Strongest Line	$\beta(J)$	Δv_Q^*	$\frac{f - \Delta v_Q}{2(J+1)}$
1→2	9,859.30 ± 0.04	-0.0607	-2.26 ± 0.03	2465.39 ± 0.01
2→3	14,792.80 ± 0.06	-0.0268	-1.00 ± 0.01	2465.63 ± 0.01
3→4	19,725.17 ± 0.01	-0.0148	-0.55 ± 0.01	2465.72 ± 0.00
4→5	24,657.26 ± 0.03	-0.0093	-0.35 ± 0.00	2465.76 ± 0.00
5→6	29,588.95 ± 0.01	-0.0063	-0.23 ± 0.00	2465.76 ± 0.00
6→7	34,520.42 ± 0.01	-0.0046	-0.17 ± 0.00	2465.76 ± 0.00

$$\Delta v_Q = \beta(J)eQV_{zz}, \text{ where } \beta(J) = -\frac{3}{4} \frac{(J+1)(J+2) + (4J+7)}{(2J+5)(2J+3)(J+2)(J+1)}$$

* $eQV_{zz} = 37.3 \pm 0.5$ mc based on $J = 1 \rightarrow 2$ data.

The increasing value of $(f - \Delta v_Q) / 2(J+1)$ with increasing J is a strange effect, if one assumes that it is the result of centrifugal stretching, because it implies a negative value of D_J . Calculations based on Table 5, the $J = 1 \rightarrow 2$ data and the $J = 2 \rightarrow 3$ through $J = 6 \rightarrow 7$ data yield for D_J the values: -0.024 ± 0.002 mc, and -0.014 mc, -0.009 mc, -0.006 mc, and -0.004 mc with probable errors less than 0.001 mc. A least squares fit for the various rotational spectra permitted the determination of a single value of D_J which provides a good prediction for locating the frequencies corresponding to the $J = 1 \rightarrow 2$ through $J = 6 \rightarrow 7$ spectra. This analysis gives

$$(B - D_{JK}) = 2465.6 \text{ mc and}$$

$$D_J = -6.6 \text{ kc.}$$

Use of D_{JK} obtained from analysis of the $J = 2 \rightarrow 3$ spectrum gives

$$B = 2465.4 \text{ mc,}$$

$$D_{JK} = -196 \pm 6 \text{ kc, and}$$

$$D_J = -6.6 \text{ kc.}$$

The standard deviation of the frequencies predicted by the equation

$$f = 2(J+1)(B - D_{JK}K^2) - 4D_J(J+1)^3 + \Delta v_Q,$$

where

$$\Delta v_Q = -\frac{3}{4} \frac{(J+1)(J+2) + (4J+7)}{(2J+5)(2J+3)(J+2)(J+1)} eQV_{zz},$$

and

$$eQV_{zz} = 37.3 \text{ mc},$$

from the set of measured frequencies in Table 5 is 0.5 mc. With this fit the largest discrepancy occurs for $J = 1$; the measured frequency is approximately one megacycle lower than is predicted with the constants obtained by the least squares fit.

Quadrupole Coupling Constant.--In order to compare the quadrupole coupling constant of fluorotrichloromethane with that of other methyl chlorides, it is convenient to express the field gradient at the chlorine nucleus V_{zz} in terms of V_{aa} , where \underline{a} is the C-Cl bond direction. If it is assumed that the field gradient is due entirely to a cylindrically symmetric charge distribution about the C-Cl bond, then (15)

$$V_{zz} = (\cos 2\alpha) V_{aa} = \frac{1}{2}(3 \cos^2 \beta - 1) V_{aa},$$

where 2α is the angle Cl-C-Cl and β is the angle between a C-Cl bond and the molecular symmetry axis. The value $109^\circ 40'$ for 2α gives

$$eQV_{aa} = -110.8 \pm 1.5 \text{ mc}$$

for the quadrupole coupling constant of CFCl_3 . Table 6 lists the quadrupole coupling constants obtained from both microwave spectra and pure quadrupole resonance studies for various methyl chlorides. Where necessary for the derivation of eQV_{aa} , the assumption of axial symmetry of charge about the C-Cl bond was made.

Table 6. The Quadrupole Coupling Constant of Cl^{35} in the Methyl Chlorides

Molecule	Gas		Solid	
	eQV_{aa}	reference	eQV_{aa}	reference
CH_3Cl	-75.50 mc	(33)	68.40 mc	(35)
CH_2Cl_2	-78.4 ± 2	(34)	72.47	(35)
CHCl_3	-80.39 ± 0.22 -102.5 ± 1.4	(15) *	76.98	(35)
CFCl_3	-110.8 ± 1.5	*	79.63	(35)
CCl_4			81.85	(35)

*Present investigation

The coupling constant for fluorotrichloromethane obtained in the present investigation does not fit the empirical sequences apparent in the table.

The possible discrepancy between the coupling constant obtained in this investigation for CFCl_3 and the constant obtained by Wolfe in an analysis of the $J = 2 \rightarrow 3$ spectrum of CHCl_3 , the only previously investigated molecule with three nuclei with spin $3/2$, was particularly disturbing. For this reason the $J = 1 \rightarrow 2$ spectrum of the most abundant symmetric top species of chloroform was examined; the measurements were made with the sample at dry ice temperature. The hyperfine structure for this spectrum was found to have the same general features as that of CFCl_3 . The two relatively strong lines were repeatedly measured; the strongest line occurred at $13,204.32 \pm 0.04$ mc and the second strongest line occurred at $13,208.89 \pm 0.05$ mc. In accordance with the discussion of the $J = 1 \rightarrow 2$ spectrum for CFCl_3 , the frequency difference of these lines is $0.1250 eQV_{zz}$. This provides

$$eQV_{zz} = 36.3 \pm 0.5 \text{ mc.}$$

Use of the conversion based on the assumption of charge symmetry about the C-Cl bond direction and the Cl-C-Cl angle of $110^{\circ}55'$ (15) gives

$$eQV_{aa} = -102.5 \pm 1.4 \text{ mc.}$$

There is a general agreement in the ratio of quadrupole coupling constant of CFCl_3 to that of CHCl_3 obtained from the pure quadrupole resonance data and the ratio of the much larger constants obtained in this investigation.

Experience with the analysis of the $J = 2 \rightarrow 3$ spectrum of CFCl_3 had indicated that it would have been virtually impossible to analyze this spectrum without the value of eQV_{zz} from the $J = 1 \rightarrow 2$ spectrum and with data from higher rotational transitions. On this basis it was decided that Wolfe's frequency data should be reviewed to ascertain if they represent a definite discrepancy with the $J = 1 \rightarrow 2$ data.

Table 7 compares measured frequencies of lines in several spectra for chloroform and the values of $f - \Delta v_Q / 2(J+1)$ similar to Table 5. The lowest measured frequency for the $J = 2 \rightarrow 3$ transition was taken from Table 2 of reference 15 to indicate that this line is indeed the most intense line for a more completely resolved spectrum. That this can happen may be seen by a comparison of Figures 8 and 9 for CFCl_3 . Wolfe's measured spectrum has two large prominences similar to those in Figure 9. If it is assumed that the lowest frequency reported by Wolfe corresponds to that of the most intense component for $K = 1$, then the second most intense $K = 1$ line would occur at $19,812.86 \pm 0.06 \text{ mc}$ (if

$eQV_{zz} = 36.6 \pm 0.5$ mc); the frequency of the strongest prominence in Wolfe's data was $19,812.92 \pm 0.10$ mc. The analysis above makes use of $K = 1$ lines only. Wolfe based his analysis on the least squares fit of lines identified with the $K = 2$ spectrum; this analysis provided the position of his most intense line. Because it was not known why the quadrupole coupling constant might change with K (or J), and since such a change was not evident in the analysis of the $J = 2 \rightarrow 3$ spectrum of $CFCl_3$, Wolfe's frequency data were further reviewed.

Table 7. Various Chloroform Lines

Transition	Measured Frequency	Ref.	$\Delta\nu_Q^*$	$\frac{f - \Delta\nu_Q}{2(J+1)}$
1 \rightarrow 2	$13,204.32 \pm 0.04$	**	-2.22 ± 0.03	3301.64 ± 0.01
2 \rightarrow 3	$19,812.92 \pm 0.10$	(15)	-0.98 ± 0.01	3302.32 ± 0.02
	$19,810.57 \pm 0.05$	(15)	-0.98 ± 0.01	3301.93 ± 0.01
6 \rightarrow 7	$46,227.2 \pm 0.15$	(36)	-0.17 ± 0.00	3301.96 ± 0.01

* $eQV_{zz} = 36.6 \pm 0.5$ mc based on $J = 1 \rightarrow 2$ data
 **Present Investigation

A good fit to most of Wolfe's data can be made with the assignment discussed above for the $K = 1$ spectrum (Figure 6) if the $K = 2$ spectrum (Figure 7) is shifted by $\Delta\nu_Q/eQV_{zz}$ equal to 0.09878. This shift corresponds to $D_{JK} = -200.9 \pm 2.9$ kc. With this assignment relatively weak lines corresponding to 13, 14, 15 (Figure 7) would occur at 19,824.66 mc, 19,826.31 mc and 19,827.77 mc; these are outside the range of frequencies reported by Wolfe. That there is a good possibility these lines actually exist may be seen by referring to the recorded spectrum in Figure 18 of

reference 24. As expected for a spectrum as complex as this one, a perfect fit will not be obtained with this procedure. It was, however, reassuring to notice that a prominent line observed by Wolfe at $19,808.28 \pm 0.12$ mc but not positively identified in his assignment (see Figure 21 of reference 24) corresponds to line d (Figure 6), which in the present assignment is located at $19,808.34 \pm 0.06$ mc.

The present investigation indicates no definite discrepancies between the eQV_{zz} for the $J = 1 \rightarrow 2$ and the $J = 2 \rightarrow 3$ spectra of $CFCl_3$ or $CHCl_3$. The values of eQV_{aa} obtained under the assumption of charge symmetry about the C-Cl bonds seem too large in comparison with the pure quadrupole data. Therefore one must conclude that the quadrupole interaction calculations common to the $J = 1 \rightarrow 2$ and $J = 2 \rightarrow 3$ spectra for three nuclei are in error by a multiplicative factor or the assumption of charge symmetry about the C-Cl bond is not valid for the case of three nuclei.

Discussion of Results

The existence of what has appeared to be a negative value of D_J is interesting because previous investigations have yielded only positive values (32), and D_J has been expected to always be positive because centrifugal stretching due to rotation about any given axis will always tend to increase the moment of inertia about that axis (32). Thomas, Cox, and Gordy (37) have, however, presented an argument which permits the existence of a negative D_J . They argue that the molecular distortion comes about principally by a change in the nature of the C-Cl bond in $CHCl_3$ with a change in angle β (Figure 1). Such

a mechanism might make the C-F bond (and the C-H bond) shorter and D_J negative. CFCl_3 and CHCl_3 are the only molecules with three nuclei of spin $3/2$ to which the theory of quadrupole interaction has been applied; they are also the only molecules for which negative values of D_J have been obtained. Effects which might produce the strange values calculated for D_J are discussed below.

One might surmise that the increasing value of $f - \Delta\nu_Q/2(J+1)$ with increasing J is caused by increasingly larger permissible K with J . Since D_{JK} is negative and D_J is expected to be small, this might shift the peak of the unresolved components of different K toward higher frequencies. Equation 14

$$\frac{f - \Delta\nu_Q}{2(J+1)} = (B - D_{JK}K^2) - 2D_J(J+1)^2$$

may be helpful to the reader. A misleading peak could result from a summation of hyperfine components of different K in a manner similar to that which causes the misleading peak in Figure 9. This explanation is untenable because of the negative value of D_J which is obtained in comparing the $J = 1 \rightarrow 2$ and $J = 2 \rightarrow 3$ spectra, for which the major $K = 1$ components are indeed resolved for both spectra.

The validity of using Equation 5 to calculate the frequency shift of the most intense line in each rotational transition might be questioned because of the large values obtained for eQV_{aa} . However, from an inspection of Tables 13 and 14 it can be seen that this equation does predict the same shifts that were calculated from Equation 5 for the $J = 1 \rightarrow 2$ and $J = 2 \rightarrow 3$ spectra. Since the measured spectra closely

resemble the spectra predicted from the matrix elements of Equation 3, Equation 5 in conjunction with the determined values of eQV_{zz} does indeed predict the correct frequency shift of the most intense line ($K = 1$) from the center of each hyperfine spectrum. This will be true even if the values of eQV_{zz} so obtained are in error by a multiplicative constant because of an error in the theoretical calculations.

The above discussion does not rule out the possibility that the center of each hyperfine spectrum may be shifted with respect to their respective rotational lines. If each $K = 1$ hyperfine spectrum were shifted downward in frequency by an amount that decreases with increasing J , the spacing between adjacent $K = 1$ spectra would change so as to give the effect of a negative value of D_J . The large and almost equal negative values of D_{JK} , obtained in the analysis of the $J = 2 \rightarrow 3$ spectra for CFCl_3 and CHCl_3 , might then indicate that there exists a shift in the centers of the hyperfine spectra which is dependent on K in addition to J .

The fundamental vibrational levels (38) for CFCl_3 , expressed in inverse centimeters are $\omega_1 = 1085$, $\omega_2 = 534$, $\omega_3 = 351$, $\omega_4 = 846$, $\omega_5 = 400$, and $\omega_6 = 245$. The first three are nondegenerate and of species A_1 , and the last three are doubly degenerate and of species E . These vibrational levels are distributed so that a relatively large number of molecules are in the first-excited vibrational state, even at dry ice temperature. The ground (ω_0) and first excited (ω_6) states have the following approximate populations:

<u>Temperature</u>	<u>ω_0</u>	<u>ω_6</u>
27°C	25%	15%
-78°C	57%	19%.

The lack of knowledge of the rotational constants for the excited vibrational states makes it impossible to quantitatively take into account the possible effects of interference from this source. Unpredicted weak recorder deflections may be produced by vibrational effects but they may also be produced by lines from other isotropic species or by weak reflections in the spectrometer.

CHAPTER V

CONCLUSIONS

A conventional Stark spectrograph is analogous to a superheterodyne detector with intermediate frequency of zero. Because of this, a crystal diode detector operated at a higher microwave power level than is usual for spectrographs will provide improved sensitivity. A crystal diode detector operating at a one to two milliwatt power level can be used at X-band with an 85-kc Stark modulation system to detect lines having absorption coefficients less than 10^{-10} cm⁻¹.

Approximate rotational constants of CFCl_3 are

$$A(\text{I}) = B(\text{I}) = 2465.39 \text{ mc}$$

for CFCl_3^{35} , and

$$A(\text{II}) = 2463.22 \text{ mc}$$

$$B(\text{II}) = 2398.50 \text{ mc}$$

for $\text{CFCl}_2^{35}\text{Cl}^{37}$. The structural parameters for CFCl_3 are:

$$\text{C-Cl} = 1.76 \text{ \AA},$$

$$\text{C-F} = 1.33 \text{ \AA}, \text{ and}$$

$$\text{Cl-C-Cl} = 109^\circ 40'.$$

Based on the quadrupole coupling theory, the quadrupole coupling constant with respect to the molecular symmetry axis, eQV_{zz} , of CFCl_3^{35}

is 37.3 ± 0.5 mc. The quadrupole coupling constant in CFCl_3^{35} with respect to the C-Cl bond, eQV_{aa} , is -110.8 ± 1.5 mc under the usual assumption that extranuclear charge is symmetric about the bond axis. The quadrupole coupling constant in CHCl_3^{35} with respect to the symmetry axis is 36.6 ± 0.5 mc; eQV_{aa} under the assumption of charge symmetry is -102.5 ± 1.4 mc.

Details of the measured $J = 1 \rightarrow 2$ and $J = 2 \rightarrow 3$ hyperfine spectra for CFCl_3^{35} and CHCl_3^{35} match the predicted hyperfine spectra. The magnitudes of the eQV_{aa} obtained for CFCl_3 and CHCl_3 are large compared with data from other methyl chlorides. There is a general agreement in the ratio of quadrupole coupling constant of CFCl_3 to that of CHCl_3 from pure quadrupole resonance data and the ratio of the larger eQV_{aa} obtained in this investigation.

Based on the existing quadrupole interaction theory, the centrifugal distortion constant D_J is negative for $K = 1$ lines and the magnitude decreases with increasing J . Frequencies for which the maximum absorption occurs in the $J = 1 \rightarrow 2$ through $J = 6 \rightarrow 7$ rotational transitions of CFCl_3^{35} indicate that the rotational constant B and the centrifugal distortion constants D_J and D_{JK} are

$$(B - D_{JK}) = 2465.6 \text{ mc and}$$

$$D_J = -6.6 \text{ kc.}$$

Use of D_{JK} obtained from the $J = 2 \rightarrow 3$ spectrum gives

$$B = 2465.4 \text{ mc,}$$

$$D_{JK} = -196 \text{ kc, and}$$

$$D_J = -6.6 \text{ kc.}$$

The large values of eQV_{aa} obtained for $CFCl_3$ and $CHCl_3$ indicate one of the following difficulties: (1) the quadrupole interaction theory is in error by a multiplicative factor, or (2) the usual assumption of charge symmetry about the C-Cl bond is not valid for this molecule. Existence of an error in the quadrupole coupling theory might explain the large values of eQV_{aa} and D_{JK} , the negative values of D_J , and the dependence of D_J on J .

CHAPTER VI

RECOMMENDATIONS

The $J = 0 \rightarrow 1$ spectrum of a molecule having three nuclei of spin $3/2$ should be investigated. CHCl_3 is preferable to CFCl_3 for this purpose because the larger dipole moment results in a greater absorption coefficient and a larger Stark displacement for the same electric field. Equipment required for the $K = 0$ spectrum must supply a large electric field because the Stark effect for $K = 0$ is of second order. Because of this the equipment should consist of a Stark modulator operating at 1000 cps or less to provide an adequate electric field strength without excessive power requirements on the Stark modulator. At this modulation frequency a bolometer detector will provide greater sensitivity than would be obtainable with a crystal detector.

Data which are better resolved than Wolfe's should be experimentally obtained for the $J = 2 \rightarrow 3$ hyperfine spectrum of CHCl_3 ³⁵.

Details of the $J = 3 \rightarrow 4$ and higher rotational transitions of CFCl_3 or CHCl_3 should be further investigated. It may be possible to associate frequencies corresponding to centers of the $K = 2$ hyperfine spectra. These frequencies, with the $K = 1$ data from the present investigation, will provide insight into a possible dependence of D_{JK} on J .

The theory of quadrupole interaction should be reinvestigated with a view toward explaining the large values of eQV_{aa} and D_{JK} , the negative values of D_J , and the dependence of D_J on J .

A P P E N D I C E S

APPENDIX A

DERIVATION FOR ADDITION OF TWO IN-PHASE WAVES

For convenience let the transmitted microwave power from the signal oscillator be represented by a voltage defined so that $V^2 = ZP$, where P is the power and Z is the guide impedance. V is the rms voltage of the wave. To further simplify the rotation, let $Z = 1$. Let a much smaller voltage, δV , from the same oscillator be added in phase with V . The power contained in the wave having amplitude $V + \delta V$ is then

$$P + \Delta P = (V + \delta V)^2 = V^2 + 2V(\delta V) + (\delta V)^2.$$

Since $V^2 = P$, the above equation gives

$$(\delta V)^2 + 2V(\delta V) - \Delta P = 0.$$

Since ΔP and δV must have the same sign, use of the quadratic equation gives

$$\delta V = -V + \sqrt{V^2 + \Delta P} = -\sqrt{P} + \sqrt{P} \left[1 + \frac{\Delta P}{P} \right]^{\frac{1}{2}}.$$

Expansion of the second term by the binomial series gives

$$\delta V = -\sqrt{P} + \sqrt{P} \left[1 + \frac{1}{2} \left(\frac{\Delta P}{P} \right) - \frac{1}{8} \left(\frac{\Delta P}{P} \right)^2 + \dots \right].$$

$P/\Delta P$ will exceed 10^6 for the cases to be considered. Then

$$\delta V \approx \frac{1}{2} \Delta P / \sqrt{P}. \tag{15}$$

Since $(\delta V)^2$ is the power of the wave having amplitude δV , P' , squaring Equation 15 gives

$$P' = \frac{(\Delta P)^2}{4P} . \quad (16)$$

To clarify the meaning of Equation 16 consider the following example of its application to the fields in a Stark cell. Let ΔP be the power absorbed by the gas and let P be the input power to a cell having negligible attenuation. Then P' is the small amount of unbalanced power which would exist due to an absorption line if one were to use r-f balancing to cancel the power when the oscillator was not at the frequency of an absorption line.

APPENDIX B

CORRECTION TO MOMENTS OF INERTIA FOR SPECIES II

Principal moments of inertia are obtained by determining the roots of the secular equation (39)

$$\begin{vmatrix} I_{xx} - I & I_{xy} & I_{xz} \\ I_{xy} & I_{yy} - I & I_{yz} \\ I_{xz} & I_{yz} & I_{zz} - I \end{vmatrix} = 0.$$

The origin in the coordinate system selected is at the molecular center of mass, z is along the molecular symmetry axis, x is in the C-F-Cl³⁷ plane and perpendicular to z, and y is perpendicular to x and z. The secular equation for this coordinate system reduces to

$$\begin{vmatrix} I_{xx} - I & 0 & I_{xz} \\ 0 & I_{yy} - I & 0 \\ I_{xz} & 0 & I_{zz} - I \end{vmatrix} = 0.$$

In the notation for asymmetric top molecules ($I_A < I_B < I_C$), the principal moments of inertia obtained from the secular equation are

$$I_A = \frac{(I_{xx} + I_{zz})}{2} - \frac{(I_{xx} - I_{zz})}{2} \sqrt{1 + \frac{4I_{xz}^2}{(I_{xx} - I_{zz})^2}}$$

$$I_B = I_{yy}$$

$$I_C = \frac{(I_{xx} + I_{zz})}{2} + \frac{(I_{xx} - I_{zz})}{2} \sqrt{1 + \frac{4I_{xz}^2}{(I_{xx} - I_{zz})^2}} .$$

Let

$$\Delta = \frac{4I_{xz}^2}{(I_{xx} - I_{zz})^2} ;$$

then for $\Delta \ll 1$, the principal moments of inertia are

$$I_A = I_{xx} - \frac{I_{xz}^2}{(I_{zz} - I_{xx})} ,$$

$$I_B = I_{yy}, \text{ and}$$

$$I_C = I_{zz} + \frac{I_{xz}^2}{(I_{zz} - I_{xx})} .$$

APPENDIX C

RACAH COEFFICIENTS

Most of the coefficients used for calculation of the $J = 1 \rightarrow 2$ spectrum were obtained from published tables (40,41). The remainder were obtained by hand from Equation 17 below and the tables by Sharpe et al (40). The following discussion was taken from the aforementioned report by Sharpe.

The Racah coefficient $W(abcd,ef)$ arises in the relationship between different ways of combining the vectors a , b , and d to give a resultant c . In terms of Clebsch-Gordan coefficients, this relationship is:

$$(ab|e)(ed|c) = \sum_f (2e+1)^{\frac{1}{2}} (2f+1)^{\frac{1}{2}} (bd|f)(af|c)W(abcd,ef).$$

As this relationship is independent of the magnetic quantum numbers, these have been suppressed in writing the Clebsch-Gordan coefficients. An algebraic formula for $W(abcd,ef)$ has been given by Racah (26):

$$W(abcd,ef) = \Delta(abe) \Delta(cde) \Delta(acf) \Delta(bdf) w(abcd,ef) \quad (17)$$

where

$$w(abcd,ef) = \sum_z \left\{ \frac{(-1)^{a+b+c+d+z} (z+1)!}{(z-a-b-e)!(z-c-d-e)!(z-a-c-f)!(z-b-d-f)!} \times \frac{1}{(a+b+c+d-z)!(a+d+e+f-z)!(b+c+e+f-z)!} \right\}.$$

The "triangle coefficient" $\Delta(abc)$ is defined by

$$\left[\Delta(abc) \right]^z = \frac{(a+b-c)!(b+c-a)!(c+a-b)!}{(a+b+c+1)!}$$

provided a, b, c form the sides of a triangle with integral sum. Δ is symmetrical with respect to permutations of a, b, c . The sum runs over all integral values of z that do not make the arguments of factorials in the denominator negative. From either formula it follows that the Racah coefficient is defined only if each of the four triads (abe) , (cde) , (acf) , (bdf) form the sides of a triangle and have integral sum. The algebraic formula also exhibits the symmetries of W :

$$\begin{aligned} W(abcd,ef) &= W(badc,ef) = W(cdab,ef) = W(acbd,fe) \\ &= (-1)^{e+f-a-d} W(ebcf,ad) \\ &= (-1)^{e+f-b-c} W(aefd,bc). \end{aligned}$$

Any particular W can be computed rapidly using the algebraic formula together with the table of factorials in factored form given in the tables by Sharpe et al. The quantities tabulated in these tables are rational fractions which, for the ranges of parameters considered, contain prime factors larger than 19 only in exceptional cases. Since the computations required involve multiplications and divisions, this notation enables these operations to be carried on quickly.

APPENDIX D

CALCULATIONS FOR $J = 1 \rightarrow 2$ TRANSITION

Table 8. Matrix Elements for J = 1

F	S	I	I'	$\lambda(SII')$	$W(III'1;F2)$	(F - J + 1/2)	$H'_{rr'}/G(11)$
9/2	E	7/2	7/2	0.92582	0.044096	4	0.040825
7/2	E	7/2	7/2	0.92582	0.125988	3	-0.116642
		5/2	5/2	0.13094	0.044543	3	-0.005832
		7/2	5/2	-0.90712	0.094491	3	0.085715
5/2	E	7/2	7/2	0.92582	0.094491	2	0.087482
		5/2	5/2	0.13094	0.142539	2	0.018664
		3/2	3/2	1.40000	0.040825	2	0.057155
		7/2	5/2	-0.90712	0.146385	2	-0.132789
		7/2	3/2	1.38564	0.182574	2	0.252982
		5/2	3/2	1.20000	0.100000	2	0.120000
3/2	E	5/2	5/2	0.13094	0.124721	1	-0.016331
		3/2	3/2	1.40000	0.163299	1	-0.228619
		1/2	1/2	0.00000	--	1	0.000000
		5/2	3/2	1.20000	0.187082	1	-0.224498
		5/2	1/2	-0.64808	0.223606	1	0.144915
		3/2	1/2	0.69282	0.091287	1	-0.063245
1/2	E	3/2	3/2	1.40000	0.204124	0	0.285774
		3/2	1/2	0.69282	0.288675	0	0.200000
		1/2	1/2	--	0	0	0

Table 9. $J = 1, K = 1$ Eigenvalues

F	$E_1^1/G(11)$	$B_T 7/2$	$B_T 5/2$	$B_T 3/2$	$B_T 1/2$	E_1^1/eQV_{zz}	T
9/2	0.04083	1.00	0	0	0	0.02500	a
7/2	0.04083	0.48	0.88	0	0	0.02500	b
	-0.16330	-0.88	0.48	0	0	-0.10000	c
5/2	0.32659	0.74	-0.06	0.67	0	0.19999	d
	0.12249	-0.30	0.86	0.41	0	0.07501	e
	-0.28578	-0.60	-0.51	0.62	0	-0.17500	f
3/2	0.23169	0	0.71	-0.42	0.56	0.14188	g
	-0.10404	0	-0.43	0.36	0.83	-0.06371	h
	-0.37260	0	-0.55	-0.83	0.07	-0.22817	i
1/2	0.38869	0	0	0.89	0.46	0.23802	j
	-0.10291	0	0	-0.46	0.89	-0.06302	k

Table 10. $J = 2, K = 1$ Eigenvalues
(E States)

F	$E_2^1/G(21)$	B_T 7/2	B_T 5/2	B_T 3/2	B_T 1/2	E_2^1/eQV_{zz}	T'
11/2	0.05345	1.00				-0.03571	A
9/2	0.05345	0.57	0.82			-0.03571	B
	-0.13363	0.82	-0.57			0.08928	C
7/2	0.23445	0.43	0.42	0.80		-0.15665	D
	0.00609	-0.56	0.82	-0.13		-0.00407	E
	-0.21382	0.71	0.39	-0.59		0.14286	F
5/2	0.21264	-0.57	0.60	-0.38	0.42	-0.14208	G
	0.02070	0.66	0.24	0.15	0.69	-0.01383	H
	-0.11756	0.24	0.77	0.26	-0.54	0.07855	I
	-0.27613	0.43	0.00	-0.87	-0.22	0.18450	J
3/2	0.26226	0.62	-0.52	0.57	0.15	-0.17523	K
	0.08794	-0.40	0.15	0.42	0.79	-0.05876	L
	0.00000	0.68	0.59	-0.29	0.34	0.00000	M
	-0.24330	-0.05	0.56	0.66	-0.50	0.16256	N
1/2	0.30590		-0.34	0.94		-0.20439	O
	-0.06538		0.94	0.34		0.04368	P

Table 11. Intensity Factors for $J=1 \rightarrow 2$, $K=1$

ΔF	$F(J=1)$	$R_{7/2}$	$R_{5/2}$	$R_{3/2}$	$R_{1/2}$
+1	9/2	1.540	0	0	0
	7/2	-1.110	1.415	0	0
	5/2	0.653	-0.102	0.127	0
	3/2	0	0.610	-0.916	1.095
	1/2	0	0	0.578	-0.817
0	9/2	0.880	0	0	0
	7/2	-1.010	0.755	0	0
	5/2	0.876	-0.855	0.600	0
	3/2	0	0.748	-0.653	0.366
	1/2	0	0	0.577	0
-1	9/2	0.394	0	0	0
	7/2	-0.652	0.309	0	0
	5/2	0.897	-0.490	0.200	0
	3/2	0	0.634	-0.258	0

Table 12. Racah Coefficients Needed for Intensities

$W(1F2F'; I1)$	$I = 7/2$	$I = 5/2$	$I = 3/2$	$I = 1/2$
$W(1 \frac{3}{2} \ 2 \ \frac{1}{2}; I1)$	0	0.224	-0.091	0
$W(1 \frac{3}{2} \ 2 \ \frac{3}{2}; I1)$	0	0.187	-0.163	0.091
$W(1 \frac{3}{2} \ 2 \ \frac{5}{2}; I1)$	0	0.125	-0.187	0.224
$W(1 \frac{5}{2} \ 2 \ \frac{3}{2}; I1)$	0.183	-0.100	0.048	0
$W(1 \frac{5}{2} \ 2 \ \frac{5}{2}; I1)$	0.146	-0.143	0.100	0
$W(1 \frac{5}{2} \ 2 \ \frac{7}{2}; I1)$	0.094	-0.146	0.183	0
$W(1 \frac{7}{2} \ 2 \ \frac{5}{2}; I1)$	-0.094	0.045	0	0
$W(1 \frac{7}{2} \ 2 \ \frac{7}{2}; I1)$	-0.126	0.094	0	0
$W(1 \frac{7}{2} \ 2 \ \frac{9}{2}; I1)$	-0.124	0.158	0	0
$W(1 \frac{9}{2} \ 2 \ \frac{7}{2}; I1)$	0.044	0	0	0
$W(1 \frac{9}{2} \ 2 \ \frac{9}{2}; I1)$	0.088	0	0	0
$W(1 \frac{9}{2} \ 2 \ \frac{11}{2}; I1)$	0.141	0	0	0
$W(1 \frac{1}{2} \ 2 \ \frac{3}{2}; I1)$	0	0	0.204	-0.289
$W(1 \frac{1}{2} \ 2 \ \frac{1}{2}; I1)$	0	0	0.289	0

Table 13. Calculated Spectrum, $J=1 \rightarrow 2$, $K=1$

Transition (TT')	$\Delta v_Q/eQV_{zz}$	Intensity	Transition (TT')	$\Delta v_Q/eQV_{zz}$	Intensity
jO	-0.44241	0.24	hO	-0.14068	0.00
jK	-0.41325	0.08	eL	-0.13377	0.01
dK	-0.37522	0.17	dI	-0.12144	0.09
dD	-0.35664	0.08	kK	-0.11221	0.08
gO	-0.34627	0.00	hK	-0.11152	0.01
dG	-0.34207	0.24	gP	-0.09820	0.21
gK	-0.31711	0.01	eH	-0.08884	0.10
jL	-0.29678	0.00	eE	-0.07908	0.00
gG	-0.28396	0.14	hG	-0.07837	0.12
dL	-0.25875	0.04	jN	-0.07546	0.35
eK	-0.25024	0.01	eM	-0.07501	0.20
jM	-0.23802	0.10	gI	-0.06333	0.01
eD	-0.23166	0.01	aB	-0.06071	0.25
eG	-0.21709	0.14	bB	-0.06071	0.52
dH	-0.21382	0.37	aA	-0.06071	2.37
dE	-0.20406	0.14	dF	-0.05713	0.08
gL	-0.20064	0.12	cD	-0.05665	0.29
dM	-0.19999	0.19	cG	-0.04208	0.06
jP	-0.19434	0.03	bH	-0.03883	0.02
bD	-0.18165	0.01	dN	-0.03743	0.01
aD	-0.18165	0.00	bE	-0.02907	0.67
bG	-0.16708	0.12	aE	-0.02907	0.05
gH	-0.15571	0.35	dJ	-0.01549	0.00
gM	-0.14188	0.01	fK	-0.00023	0.15
kO	-0.14137	0.06			

Table 13. Calculated Spectrum, $J=1 \rightarrow 2$, $K=1$ (Continued)

Transition (TT')	$\Delta\nu_Q/eQV_{zz}$	Intensity	Transition (TT')	$\Delta\nu_Q/eQV_{zz}$	Intensity
eI	0.00354	0.32	bJ	0.15950	0.02
kL	0.00426	0.50	fH	0.16117	0.03
hL	0.00495	0.01	iL	0.16941	0.04
fD	0.01835	0.01	fE	0.17093	0.06
gN	0.02068	0.14	fM	0.17500	0.07
iO	0.02378	0.10	cI	0.17855	0.06
fG	0.03292	0.18	cC	0.18928	0.17
gJ	0.04262	0.23	iH	0.21434	0.01
hH	0.04988	0.26	kN	0.22558	0.02
iK	0.05294	0.27	hN	0.22627	0.23
bI	0.05355	0.02	iM	0.22817	0.15
kM	0.06302	0.03	cF	0.24286	0.60
hM	0.06371	0.00	hJ	0.24821	0.08
bC	0.06428	1.32	fI	0.25355	0.10
aC	0.06428	0.52	iP	0.27185	0.07
cB	0.06429	1.25	cJ	0.28450	0.06
eF	0.06785	0.02	fF	0.31786	0.10
iG	0.08609	0.21	iI	0.30672	0.01
cH	0.08617	0.17	fN	0.33756	0.06
eN	0.08755	0.03	fJ	0.35950	0.30
cE	0.09593	0.04	iN	0.39073	0.01
kP	0.10670	0.01	iJ	0.41267	0.35
hP	0.10739	0.08			
eJ	0.10949	0.10			
fL	0.11624	0.10			
aF	0.11786	0.08			
bF	0.11786	0.01			
hI	0.14226	0.61			

APPENDIX E

PREDICTED PROMINENCES FOR $J = 2 \rightarrow 3$ TRANSITION

Table 14. Predicted Prominences for $J = 2 \rightarrow 3$, $K = 1$

$\Delta v_Q/eQV_{zz}$	Relative Intensity	Designation	$\Delta v_Q/eQV_{zz}$	Relative Intensity	Designation
-0.25822	3		0.00278	52	
-0.25277	2		0.00516	66	
-0.24884	4		(0.00410)	(118)	i
(-0.25283)	(9)	a			
			0.03575	113	
-0.21903	2		0.03603	82	
-0.21496	5		(0.03586)	(195)	j
-0.20873	11				
-0.20521	5		0.04464	83	k
-0.19554	3				
(-0.20853)	(26)	b	0.08162	46	l
-0.11395	22		0.10632	65	m
-0.11091	11				
(-0.11294)	(33)	c	0.14559	14	
			0.14794	20	
-0.08781	99	d	(0.14697)	(34)	n
-0.02679	288	e	0.16074	21	
			0.16562	10	
-0.02143	59	f	(0.16232)	(31)	o
-0.01498	46	g	0.22322	17	
			0.23022	2	
-0.00697	2		0.24035	6	
-0.00686	1		0.24187	2	
-0.00620	14		0.24416	2	
-0.00559	7		(0.22999)	(29)	p
-0.00496	11				
(-0.00574)	(35)	h			

Note: Close multiplets are grouped and are considered as a single component whose intensity is the sum of the component intensities, and whose frequency is the intensity-weighted mean of the component frequencies. The resultant frequency and intensity for these groups are given in parentheses beneath the group.

Table 15. Predicted Prominences for $J = 2 \rightarrow 3$, $K = 2$

$\Delta v_Q / eQV_{zz}$	Relative Intensity	Designation
-0.40878	19	1
-0.35045	39	2
-0.31327	78	3
-0.28415	58	4
-0.11751	39	5
-0.07143	214	6
-0.02766	58	7
-0.00815	78	8
0.00000	39	9
0.08735	19	10
0.15710	58	11
0.17855	97	12
0.28573	78	13
0.32512	39	14
0.36899	58	15

BIBLIOGRAPHY

1. R. H. Hughes and E. B. Wilson, Physical Review, 71, 562 (1947).
2. Y. Beers, Theory of the Cavity Microwave Spectrometer and Molecular Frequency Standard, New York University, Report No. TN-58-871, 12 September 1958.
3. C. H. Townes and A. L. Schawlow, Microwave Spectroscopy, McGraw-Hill Book Company, Inc., New York, 1955, p. 491.
4. F. Sterzer, Journal of Chemical Physics, 22, 2094L (1954).
5. M. E. Brodwin, C. M. Johnson, and W. M. Waters, 1953 Institute of Radio Engineers Convention Record, pt 10, "Microwaves," pp. 52-57.
6. R. L. Cosgriff, A Study of Detectors and Amplifiers Used in Antenna Instrumentation, Technical Report 487-5, December 1953, Antenna Laboratory, Ohio State University Research Foundation.
7. J. H. Richmond, Transactions of the Institute of Radio Engineers, Microwave Theory and Techniques, April 1955, pp. 13-15.
8. G. Feher, Bell System Technical Journal, March 1957, p. 472.
9. H. C. Torrey and C. A. Whitmer, Crystal Rectifiers, Volume 15, Radiation Laboratory Series, McGraw-Hill Book Company, Inc., New York, 1948, p. 23.
10. PRD Microwave Test Equipment Catalog E-8, Polytechnic Research and Development Company, Inc., New York, 1958.
11. C. H. Townes and A. L. Schawlow, Microwave Spectroscopy, McGraw-Hill Book Company, Inc., New York, 1955, p. 492.
12. H. Misra, Unpublished Ph.D. Thesis, Stanford University (1957).
13. W. Gordy, W. V. Smith, and R. F. Trambarulo, Microwave Spectroscopy, John Wiley and Sons, Inc., New York, 1953.
14. Ibid, pp. 116-121.
15. P. N. Wolfe, Journal of Chemical Physics, 25, 976-981 (1956).
16. R. Livingston, Physical Review, 82, 289 (1951).
17. P. W. Allen and L. E. Sutton, Acta Crystallographica, 3, 46 (1950).

18. C. H. Townes and A. L. Schawlow, Microwave Spectroscopy, McGraw-Hill Book Company, Inc., New York, 1955, p. 55
19. R. Bersohn, Unpublished Ph.D. Thesis, Harvard University (1949).
20. M. Mizushima and T. Ito, Journal of Chemical Physics, 19, 739 (1951).
21. G. F. Hadley, Unpublished Ph.D. Thesis, Harvard University (1955).
22. S. Kojima, et al, Journal of Chemical Physics, 20, 804 (1952).
23. G. Herrmann, Journal of Chemical Physics, 22, 2093L (1954).
24. P. N. Wolfe, Unpublished Ph.D. Thesis, Ohio State University (1955).
25. G. Herrmann, Unpublished Ph.D. Thesis, New York University (1956).
26. G. Racah, Physical Review, 63, 438 (1942).
27. Townes and Schawlow, Microwave Spectroscopy.
28. W. Low and C. H. Townes, Physical Review, 76, 1295 (1949).
29. A. A. Maryott and F. Buckley, Table of Dielectric Constants and Electric Dipole Moments of Substances in the Gaseous State, National Bureau of Standards Circular 537, June 25, 1953.
30. P. Kisliuk and C. H. Townes, Molecular Microwave Spectra Tables, National Bureau of Standards Circular 518, June 23, 1952.
31. Wolfe, Unpublished Ph.D. Thesis, Tables 18 and 19.
32. Townes and Schawlow, Microwave Spectroscopy, p. 79.
33. R. Karplus and A. H. Sharbaugh, Physical Review, 75, 889 (1949).
34. R. J. Myers and W. D. Gwinn, Journal of Chemical Physics, 20, 1420 (1950).
35. R. Livingston, Journal of Chemical Physics, 19, 1434 (1951).
36. R. R. Unterberger, R. Trambarulo, and W. V. Smith, Journal of Chemical Physics, 18, 565 (1950).
37. W. J. O. Thomas, J. T. Cox, and W. Gordy, Journal of Chemical Physics, 22, 1718 (1954).
38. R. B. Bernstein, J. P. Zietlow, and F. F. Cleveland, Journal of Chemical Physics, 21, 1778 (1953).

39. H. Goldstein, Classical Mechanics, Addison-Wesley Publishing Company, Inc., Cambridge Massachusetts, 1955, p. 154.
40. W. T. Sharpe, et al, Tables of Coefficients for Angular Distribution Analysis, Atomic Energy of Canada Limited Report No. CRT-556, 4 August 1954.
41. A. Simon, J. H. Vander Suis and L. C. Biedenharn, Tables of the Racah Coefficients, Oak Ridge National Laboratory Publication No. ORNL 1679, April 1954.

VITA

Maurice Wayne Long was born on April 20, 1925, in Madisonville, Kentucky, the son of Maurice K. and Martha N. Long. He was married in 1950 to Miss Patricia Lee Holmes, and has two children.

He attended public schools in Jacksonville, Florida, and completed his studies at Robert E. Lee High School there early in 1943. He entered Stetson University in the spring of 1943 and was assigned by the U. S. Navy to the college training program at the Georgia Institute of Technology in July 1943. He remained in the training program until November 1945 and was discharged from the U. S. Navy in the spring of 1946.

He then worked as a radio engineer for a short time in Jacksonville, Florida, and returned to complete the requirements for a B.E.E. degree from Georgia Institute of Technology late in 1946. He received the M.S.E.E. degree from the University of Kentucky in 1948, spent a year in graduate studies at Columbia University and received the degree of M.S. in Physics from the Georgia Institute of Technology in 1957.

Mr. Long was employed for part of 1946 and 1947 and the summer of 1948 as a research assistant at the Georgia Institute of Technology. From 1947 to 1949 he was an instructor of electrical engineering and research associate at the University of Kentucky. Since 1950 he has been at the Engineering Experiment Station of the Georgia Institute of Technology where he is presently head of the Radar Branch.